



AKADÉMIAI KIADÓ

Central European Geology

64 (2021) 1, 18–37

DOI:

10.1556/24.2021.00001

© 2021 The Author(s)

ORIGINAL RESEARCH PAPER




[†]The first two authors have contributed equally to this work.

*Corresponding author. 'Vulcano' Petrology and Geochemistry Research Group, Department of Mineralogy, Geochemistry and Petrology, University of Szeged, Egyetem u. 2., H-6722 Szeged, Hungary.
E-mail: kiri.luca@gmail.com



Timing of magmatism of the Ditrău Alkaline Massif, Romania – A review based on new U–Pb and K/Ar data

ELEMÉR PÁL-MOLNÁR^{1,2†}, LUCA KIRI^{1†*} , RÉKA LUKÁCS^{1,2}, ISTVÁN DUNKL³, ANIKÓ BATKI^{1,2}, MÁTÉ SZEMERÉDI^{1,2}, ENIKŐ ESZTER ALMÁSI¹, EDINA SOGRÍK¹ and SZABOLCS HARANGI²

¹ 'Vulcano' Petrology and Geochemistry Research Group, Department of Mineralogy, Geochemistry and Petrology, University of Szeged, Szeged, Hungary

² MTA-ELTE Volcanology Research Group, Budapest, Hungary

³ Department of Sedimentology and Environmental Geology, Geoscience Center, University of Göttingen, Göttingen, Germany

Received: August 14, 2020 • Accepted: December 21, 2020

Published online: March 25, 2021

ABSTRACT

The timing of Triassic magmatism of the Ditrău Alkaline Massif (Eastern Carpathians, Romania) is important for constraining the tectonic framework and emplacement context of this igneous suite during the closure of Paleotethys and coeval continental rifting, as well as formation of back-arc basins.

Our latest geochronological data refine the previously reported ages ranging between 237.4 ± 9.1 and 81.3 ± 3.1 Ma. New K/Ar and U–Pb age data combined with all recently (post-1990) published ages indicate a relatively short magmatic span (between 238.6 ± 8.9 Ma and 225.3 ± 2.7 Ma; adding that the most relevant U–Pb ages scatter around ~ 230 Ma) of the Ditrău Alkaline Massif. The age data complemented by corresponding palinspastic reconstructions shed light on the paleogeographic environment wherein the investigated igneous suite was formed.

The magmatism of the Ditrău Alkaline Massif could be associated with an intra-plate, rift-related extensional tectonic setting at the southwestern margin of the East European Craton during the Middle–Late Triassic (Ladinian–Norian) period.

KEYWORDS

Ditrău Alkaline Massif, geochronology, K/Ar dating, rift-related magmatism, U–Pb dating

INTRODUCTION

The Ditrău Alkaline Massif (DAM), located in the Eastern Carpathians (Romania), is an igneous suite characterized by complex structure and lithology. Since its first mention by Lilienbach (1833) the DAM has been studied, including its petrotectonic environment, petrogenetic relations and the timing of magmatism (e.g. Koch, 1876, 1879; Streckeisen, 1938, 1960; Codarcea et al., 1957, 1958; Bagdasarian, 1972; Streckeisen and Hunziker, 1974; Pál-Molnár and Árvai-Sós, 1995; Dallmeyer et al., 1997; Krätner and Bindea, 1998; Morogan et al., 2000; Pál-Molnár, 2000, 2010a; Pană et al., 2000; Batki et al., 2004, 2014, 2018; Fall et al., 2007; Pál-Molnár et al., 2015a, 2015b).

Several analyses have been conducted with various dating methods (e.g., K/Ar, $^{40}\text{Ar}/^{39}\text{Ar}$ and U–Pb age determinations) on different rock types and mineral phases of the Ditrău Alkaline Massif. The interpretation of the results led to contradictory hypotheses on the genesis of the igneous complex and its rock associations. In order to better understand the evolution and magmatic processes of the massif, these data needed to be reconsidered and supplemented by additional, up-to-date age determination.

The aim of our study – based on the revision of previous age data and interpretation of new amphibole and biotite K/Ar, as well as titanite and zircon U–Pb ages of amphibole- and pyroxene-rich cumulate, syenite, nepheline syenite and granite samples – is to review and specify the age, time span and sequence of the open-system magmatic processes (e.g., Batki et al., 2018) that played an important role in the formation of the Ditrău Alkaline Massif.

GEOLOGIC SETTING

The Ditrău Alkaline Massif is located in the southern and southwestern part of the Giurgeu Mountains (Eastern

Carpathians, Romania) and crops out in an area of ca. 225 km² (Fig. 1A). The DAM consists of diverse rock types in an elaborate structural relationship. The most common rock types of the massif are as follows: mafic-ultramafic cumulates (e.g., hornblendite, olivine-rich cumulate, amphibole- and pyroxene-rich cumulate, amphibole-rich cumulate), alkali gabbro, alkali diorite, monzodiorite, monzonite, monzosyenite, syenite, nepheline syenite, quartz syenite and alkali granite (Fig. 1B). These rocks are cross-cut by lamprophyre, tinguaitite and syenite dykes (Pál-Molnár, 2000; Batki et al., 2014; Pál-Molnár et al., 2015a, 2015b).

The DAM had intruded into the Mesozoic crystalline rocks of the Eastern Carpathians and was subjected to nappe-forming Alpine tectonic events (Pál-Molnár, 1994a,

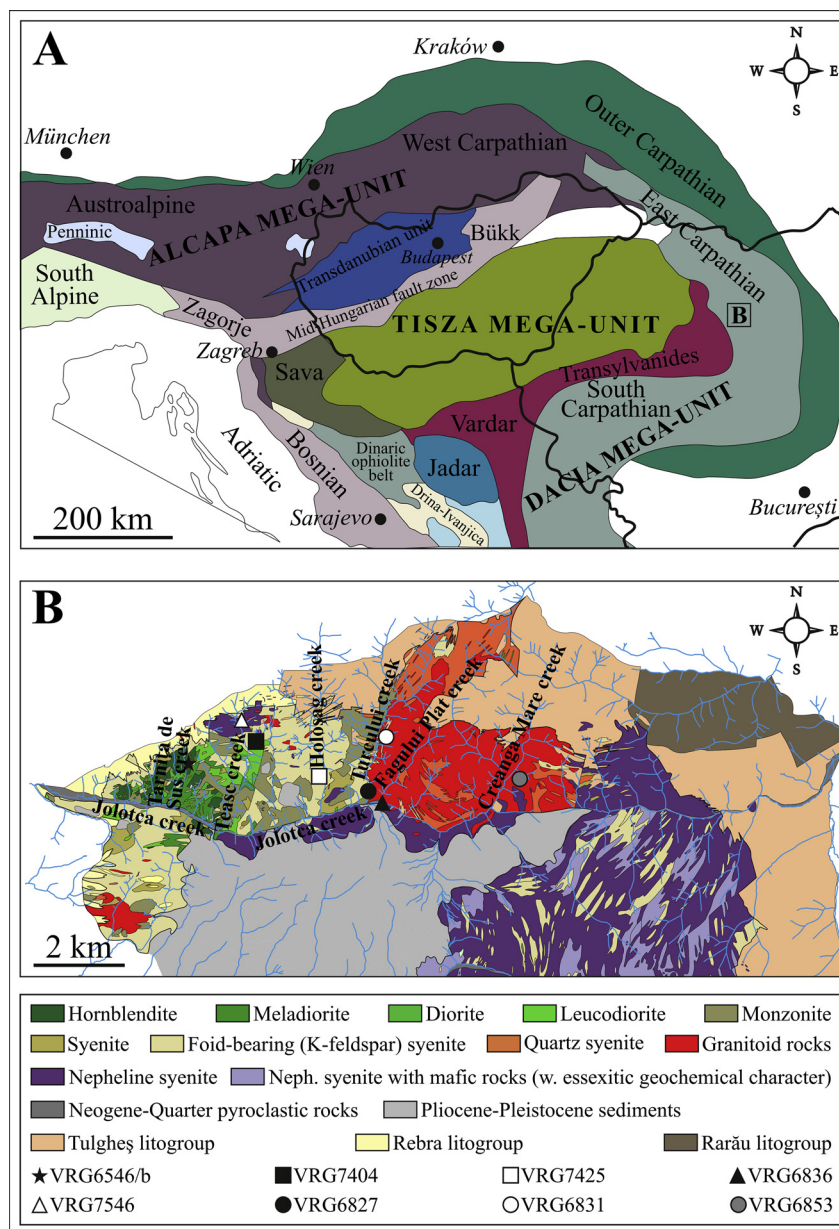


Fig. 1. (A) Location of the Ditrău Alkaline Massif (marked by a black rectangle) in the structural system of the Alpine–Carpathian–Dinaric region (after Pál-Molnár, 2010a). (B) Geologic map of the northern part of the Ditrău Alkaline Massif, displaying sample locations (Pál-Molnár et al., 2015b)

1994b; Pál-Molnár and Árvai-Sós, 1995). The Central Eastern Carpathian Zone or Crystalline Mesozoic Zone is an east-verging nappe system that was formed during the Austrian tectogenesis. It derives from the marginal part of the Getic microcontinent that forms the basement of the Transylvanian Basin. The nappe system is referred to as Median Dacides (Săndulescu, 1984) or Eastern Getides (Balintoni, 1997). According to Săndulescu (1984), the Median Dacides can be divided into three Alpine nappes (Infrabucovinian, Subbucovinian and Bucovinian), composed of pre-Alpine metamorphic rocks and Permo-Mesozoic cover sequences. Pre-Alpine, west-verging, petrographically uniform tectonic units of the Subbucovinian and Bucovinian Nappes and their respective metamorphic terranes (or alternatively: litogroups) are as follows: Rodna (Rebra Terrane), Pietrosu Bistriței (Negrișoara Terrane), Putna (Tulgheș Terrane) and Rarău Nappe (Bretila Terrane and Hăghimaș Granitoids) (Balintoni et al., 1983; Vodă and Balintoni, 1994; Balintoni, 1997).

The Ditrău Alkaline Massif belongs structurally to the Bucovinian Nappe and is in direct contact with four of its pre-Alpine metamorphic units (Bretila, Tulgheș, Negrișoara and Rebra Terrane) (Fig. 2) (Pál-Molnár, 2000; Pál-Molnár, 2010b). The massif was uprooted during the Alpine tectonic events and cut by the Bucovinian shear zone at a depth of ca. 1800–2000 m. Hence, the Subbucovinian Nappe and the DAM are bounded by a tectonic unconformity (Kräutner and Bindea, 1995).

TIMING OF THE DITRĂU MAGMATISM – PREVIOUS WORK

Early investigations – based on field and structural observations (e.g., Reinhardt, 1911; Streckeisen, 1952, 1954; Codarcea et al., 1957) – were complemented and specified by modern instrumental analytical techniques providing more precise data (Table 1). Sample locations of former studies are either unknown, or the descriptions are constrained to the name of valleys alone. Since the previous sampling points are not accurately retraceable, these data are not marked on the geologic map.

The first K/Ar dating of whole rock samples (hornblende, syenite, granite, nepheline syenite) was carried out by Bagdasarjan (1972): hornblende yielded K/Ar mean ages of 196 ± 6 – 161 ± 2 Ma. The age of syenite ranges between 142 ± 7 and 121.5 ± 0.5 Ma. Granite was suggested to be formed 125 ± 10 Ma ago. Nepheline syenite gave a K/Ar age of 152 ± 1 Ma.

According to the results of Streckeisen and Hunziker (1974), the K/Ar ages of biotite crystals from nepheline syenite are 153 ± 3 and 151 ± 9 Ma. An age of 150 ± 6 Ma was determined for the biotite of the contact metamorphic rock (hornfels). Whole rock samples of tinguaita yielded K/Ar ages of 161 ± 7 and 156 ± 6 Ma. In their hypothesis, Streckeisen and Hunziker (1974) assumed the following formation sequence for the different rock types of the massif:

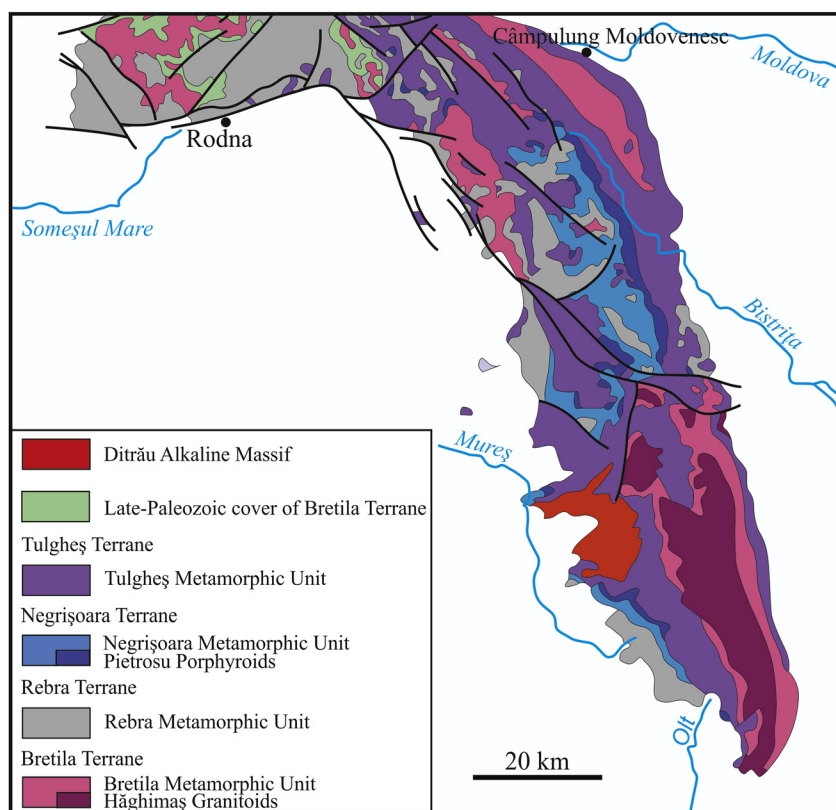


Fig. 2. Lithologic map of the pre-Alpine tectonic units of the Eastern Carpathians (after Kräutner, 1996–1997; Balintoni, 1997; Balintoni and Balica, 2013; Balintoni et al., 2014)

Table 1. Results of previously conducted age determinations

Source	Rock type	Locality	Method	Studied sample	Age (Ma)
Bagdasarian (1972)	Hornblendite	West of the conjunction of Teasc and Jolotca creeks	K/Ar	whole rock	196 ± 6
	Hornblendite	West of the conjunction of Jolotca and Simo creeks	K/Ar	whole rock	161 ± 2
	Hornblendite	West of the conjunction of Jolotca and Holoşag creeks	K/Ar	whole rock	161 ± 10
	Hornblendite	Ditrău-valley and the spring area of the Putna creek	K/Ar	whole rock	177 ± 1
	Syenite	East from the conjunction of Jolotca and Simo creeks	K/Ar	whole rock	128 ± 3
	Syenite	Central part of the Jolotca-valley	K/Ar	whole rock	121 ± 2
	Syenite	Road between Ditrău-valley and Putna creek	K/Ar	whole rock	121.5 ± 0.5
	Syenite pegmatite	East of the conjunction of Teasc and Jolotca creeks	K/Ar	whole rock	142 ± 7
	Nepheline syenite	Road between Ditrău-valley and Putna creek	K/Ar	whole rock	152 ± 1
	Leucogranite	Conjunction of Jolotca and Hompot creeks	K/Ar	whole rock	125 ± 10
	Mica schist	Basin of Putna creek, Ditrău-Tulgheş road, km 20	K/Ar	whole rock	284 ± 14
Streckeisen and Hunziker (1974)	Nepheline syenite	Comarnic plateau	K/Ar	biotite	151 ± 9
	Nepheline syenite	Ditrău creek, gallery I.	K/Ar	biotite	153 ± 3
	Tinguaite	Cianodul, 500 m E	K/Ar	whole rock	161 ± 7
	Tinguaite	Prişca, 500 m NE	K/Ar	whole rock	156 ± 6
	Hornfels	Teasc creek, 750 m SE	K/Ar	biotite	150 ± 6
Mînzatu and Ardeleanu (1980); Mînzatu et al. (1981)	Biotitized hornblendite	Jolotca-valley	K/Ar	biotite	161.0 ± 6.3
	Biotite hornblendite	Jolotca-valley	K/Ar	biotite	134.5 ± 5.2
	Biotite syenite	Ditrău-valley	K/Ar	whole rock	112
				biotite	117
	Biotite syenite	Ditrău-valley, gallery VII.	K/Ar	whole rock	131
				biotite	134.3 ± 4.8
	Biotite syenite	Ditrău-Tulgheş road, km 11	K/Ar	whole rock	136
				biotite	139.3 ± 5.1
	Biotite syenite	Ditrău-valley, quarry	K/Ar	biotite	113.6 ± 4.6
	Syenite pegmatite	Hereb-valley, gallery VI.	K/Ar	muscovite	161.8 ± 6.1
	Biotite syenite with cancrinite	Cianodul-valley	K/Ar	biotite	126.0 ± 5.0
	Syenite with sodalite (vein)	Ditrău-Tulgheş road, km 7	K/Ar	biotite	120.0 ± 4.5
	Nepheline syenite	Ditrău-valley	K/Ar	nepheline	150.9 ± 5.8
	Pegmatoidic nepheline syenite	Ditrău-valley, quarry	K/Ar	nepheline	116.1 ± 4.4
	Nepheline syenite with cancrinite	Ditrău-valley	K/Ar	nepheline	147.4 ± 6.0
	Nepheline syenite with cancrinite	Ditrău-valley	K/Ar	biotite	136.9 ± 5.1
	Liebneritized nepheline syenite	Ditrău-valley	K/Ar	nepheline	81.3 ± 3.1
	Aplite granite	Borehole 120, m 2	K/Ar	whole rock	141.9 ± 5.5
	Tinguaite	Conjunction of Aurora and Belcina creeks	K/Ar	whole rock	172.0 ± 6.6
	Tinguaite	Aurora-valley	K/Ar	whole rock	159.3 ± 6.1
	Tinguaite	Cianodul-valley	K/Ar	whole rock	141.9 ± 5.5
	Biotite hornfels	Aurora, borehole F 144.	K/Ar	whole rock	138
	Biotite hornfels	Aurora-valley, gallery VII.	K/Ar	whole rock	172
	Phlogopite marble	Lazarea, borehole, 141, m	K/Ar	biotite	150.0 ± 6.0



Table 1. Continued

Source	Rock type	Locality	Method	Studied sample	Age (Ma)
Pál-Molnár and Árvá-Sós (1995)	Hornblendite with textural ordering	Jolotca, Tarnița de Sus creek	K/Ar	amphibole	237.4 ± 9.1
	Hornblendite with textural ordering	Jolotca, Pietrarilor creek	K/Ar	amphibole	216.0 ± 8.8
	Hornblendite without textural ordering	Jolotca, gallery VI.	K/Ar	amphibole	226.0 ± 9.6
	Pegmatoidic hornblendite	Jolotca, Tarnița de Sus creek, gallery XXV.	K/Ar	amphibole	234.7 ± 10.8
				plagioclase	161.3 ± 9.8
				biotite	162.4 ± 6.1
				biotite	168.3 ± 7.2
	Meladiorite with textural ordering	Jolotca, Teasc creek	K/Ar	amphibole	208.3 ± 8.3
				feldspar	138.2 ± 5.8
	Diorite with textural ordering	Jolotca, Teasc creek	K/Ar	amphibole	176.6 ± 6.7
				feldspar	137.4 ± 5.5
	Diorite with feldspar aggregates	Jolotca, Tarnița de Jos creek	K/Ar	amphibole	218.7 ± 8.3
				feldspar	155.4 ± 5.8
	Syenite	Jolotca, Teasc creek, gallery XIX.	K/Ar	biotite	107.6 ± 4.1
				K-feldspar	182.7 ± 6.9
				biotite	102.6 ± 4.0
	Alkaline feldspar syenite	Jolotca, Simo creek	K/Ar	K-feldspar	113.5 ± 4.3
	Sodalite nepheline syenite	Jolotca, Teasc creek	K/Ar	biotite	182.4 ± 6.9
				nepheline + sodalite	232.7 ± 8.8
	Granite	Jolotca, Turcului creek	K/Ar	biotite	217.6 ± 8.3
				feldspar	146.0 ± 5.6
	Granite	Jolotca, Teasc creek	K/Ar	biotite	213.5 ± 8.2
	Granite	Jolotca, Creanga Mare creek	K/Ar	K-feldspar	139.1 ± 5.4
				biotite	206.3 ± 7.8
Dallmeyer et al. (1997)	Gabbro	Jolotca-valley	$^{40}\text{Ar}/^{39}\text{Ar}$	K-feldspar	142.7 ± 5.7
	Hornblende diorite	Ditrău-Tulgheș road, km 7	$^{40}\text{Ar}/^{39}\text{Ar}$	amphibole	227.1 ± 0.1
Pană et al. (2000)	Syenite	Jolotca, Jolotca creek	U–Pb	amphibole	231.5 ± 0.1
				zircon	229.6 ± 1.7/ –1.2

(1) intrusion of dioritic and gabbroic magmas into the crystalline country rocks; (2) intrusion of syenitic magma and formation of granitoid rocks by assimilation in the marginal zones of the massif; (3) intrusion of nepheline syenite magma, accompanied by metasomatism and hybridization; (4) formation of lamprophyre, pegmatite and aplite dykes.

Considering the results of formerly conducted K/Ar age determinations, Kräutner et al. (1976) assumed that the emplacement age of the DAM is 135 Ma.

Mînzatu and Ardeleanu (1980), as well as Mînzatu et al. (1981) performed K/Ar analyses on minerals and whole rock samples as well. Muscovite separated from syenite yielded a K/Ar age of 161.8 ± 6.1 Ma, whereas the age of biotite ranges between 139.3 ± 5.1 and 113.6 ± 4.6 Ma. Whole rock samples of syenite gave K/Ar ages of 136 – 112 Ma. The ages of biotite of metasomatically altered syenite are 126.0 ± 5 and 120.0 ± 4.5 Ma. An age of 141.9 ± 5.5 Ma was obtained for whole rock samples of granite aplite. Biotite of hornblendite yielded K/Ar ages of 161.0 ± 6.3 and 134.5 ± 5.2 Ma. Measured ages of nephelines from nepheline syenite are 150.9 ± 5.8 and 116.1 ± 4.4 Ma. Biotite of metasomatically

altered nepheline syenite gave a K/Ar age of 136.9 ± 5.1 Ma, while the ages of nephelines are 147.4 ± 6 and 81.3 ± 3.1 Ma. Whole rock ages of tinguaites range from 172.0 ± 6.6 to 141.9 ± 5.5 Ma. Whole rock samples of the contact rock (hornfels) yielded a K/Ar age of 138 Ma, whereas the age of biotite is 156.8 ± 5.9 Ma.

Based on Popescu (1985), the Rb–Sr whole rock age of ultrabasic rocks and syenite is 200 and 160 Ma, respectively.

Zincenco (1991) reinterpreted the available K/Ar and Rb–Sr data. According to his hypothesis, the DAM entered the subsolidus stage 171 ± 3 Ma ago. Pneumatolytic and hydrothermal phases ended 165 ± 5 and 154 Ma ago, respectively. Based on supplementary Rb–Sr whole rock data, Zincenco et al. (1994) proposed an emplacement age of 201 ± 1 Ma.

Pál-Molnár and Árvá-Sós (1995) determined the K/Ar age of minerals of different rock types (cumulate rocks, diorite, granite, nepheline syenite, syenite and alkaline feldspar syenite). Amphiboles of cumulate rocks gave K/Ar ages of 237.4 ± 9.1 – 216.0 ± 8.8 Ma. Amphiboles of diorite display various ages between 218.7 ± 8.3 and 176.6 ± 6.7 Ma. The obtained K/Ar age of biotite and feldspar of syenite is 107.6 ± 4.1 and 182.7 ± 6.9 Ma, respectively. Biotite and

alkaline feldspar of alkaline feldspar syenite yielded a K/Ar age of 102.6 ± 4 and 113.5 ± 4.3 Ma, respectively. Biotite and nepheline + sodalite of sodalite nepheline syenite reached their closure temperature at 182.4 ± 6.9 and 232.7 ± 8.8 Ma, respectively. K/Ar ages of biotite of granite range from 217.6 ± 8.3 to 206.3 ± 7.8 Ma, whereas the age of alkaline feldspar is 142.7 ± 5.7 – 139.1 ± 5.4 Ma. Based on the above results, Pál-Molnár and Árvai-Sós (1995) developed a two-stage evolution history for the massif: (1) Middle Triassic–Lower Jurassic (hornblende, nepheline syenite, granite); (2) Middle Jurassic–Lower Cretaceous (syenite, alkaline feldspar syenite, diorite).

Dallmeyer et al. (1997) estimated the age of hornblende with the $^{40}\text{Ar}/^{39}\text{Ar}$ method. The $^{40}\text{Ar}/^{39}\text{Ar}$ plateau age of amphibole from hornblende and gabbro is 231.5 ± 0.1 and 227.1 ± 0.1 Ma, respectively.

Copious age data by Bagdasarian (1972), Streckeisen and Hunziker (1974), Kräutner et al. (1976), Mînzatu and Ardeleanu (1980), Mînzatu et al. (1981), Popescu (1985), Zincenco (1991), Zincenco et al. (1994), Pál-Molnár and Árvai-Sós (1995), and Dallmeyer et al. (1997) were summarized and interpreted by Kräutner and Bindea (1998). According to their hypothesis, the DAM was formed by a five-stage magmatic process: (1) generation of a mantle-derived gabbroic-dioritic magma in an extensional tectonic environment (at 230 Ma); (2) 215 Ma ago the subsolidus gabbroic-dioritic magma intruded into the crust and interacted with the crustal syenitic melt. Hybrid rocks were formed as a consequence of magma mixing and mingling; (3) parental melt of nepheline syenite was formed by the opening of the Cîrcin-Severin Rift Zone (160 Ma ago). Mafic, feldspathoid-bearing rocks [ditro-essexite (alkali gabbro or monzodiorite with essexitic-theralitic chemistry)] were generated by hybridization and partial metasomatic substitution; (4) the magmatic system cooled to below 300 °C at 135 Ma. The hydrothermal activity ceased 115 Ma ago; (5) closure of the Ar-system (115 Ma) can be attributed to tectonic uplift caused by nappe transport (Kräutner and Bindea, 1998).

Pană et al. (2000) conducted U–Pb analyses on zircons of syenite; 116 separated grains were examined by Thermal Ionization Mass Spectrometry (TIMS). An age of 229.6 ± 1.7 – 1.2 Ma (Mean Square of Weighted Deviations, MSWD = 1.7) was reported for the syenite. They concluded that the syenite intruded almost at the same time as gabbro and diorite; hence the magmatic evolution of the massif was considerably shorter than previously presumed (e.g., by Pál-Molnár and Árvai-Sós, 1995; Kräutner and Bindea, 1998).

SAMPLING AND ANALYTICAL TECHNIQUES

Sampling and petrography

Eight rock samples (1 cumulate, 2 syenites, 2 nepheline syenites and 3 granites) were collected from surface outcrops of the DAM. The cumulate rock (VRG6546/b), syenite (VRG7404, VRG7425) and nepheline syenite (VRG6836,

VRG7546) were sampled in the valleys of the Târnița, Teasc, Holoșag and Fagului Plat creeks. The granite samples (VRG6827, VRG6831, VRG6853) were collected in the valleys of the Turcului and Creanga Mare creeks (Fig. 1B). Petrographic observations were carried out at the Department of Mineralogy, Geochemistry and Petrology, University of Szeged, Szeged, Hungary with optical microscopes. Mineral phases were identified with a THERMO Scientific DXR Raman microscope. Modal compositions (V/V%) in petrographic descriptions were estimated from thin sections. Radiometric age data were classified by the Geologic Time Scale of the ICS (2018/08) (Cohen et al., 2013, updated).

K/Ar geochronology

For the purpose of K/Ar age determination, the least-altered rocks were selected from more than 100 samples. Investigations were performed on separated mineral phases (amphibole and biotite) at the Institute for Nuclear Research, Hungarian Academy of Sciences, Debrecen, Hungary, using a digital flame photometer and a magnetic mass spectrometer. The Asia-1/65 Russian, GL-O French, LP-6 American and HD-B1 German reference materials were used as external standards. Given errors only represent analytical errors (standard deviation); consequently, geologic factors (e.g., Argon-loss, excess Argon) cannot be identified. Description of the equipment, methodology of the analysis and calibration of the device can be found in studies by Balogh (1985) and Odin et al. (1982).

U–Pb geochronology

Titanite (VRG7404) and zircon (VRG7425) crystals were separated from two syenite samples and from one nepheline syenite sample (VRG7546) from the northern part of the DAM (Fig. 1B). Sample preparation for U–Pb geochronology included standard gravity and magnetic separation from the 63–500 µm size fractions. Zircon and titanite crystals were mounted in epoxy resin mounts and were polished to a 1 µm finish. All mineral species were investigated and mapped by optical microscopy, cathodoluminescence (CL) and back-scattered (BSE) imaging. CL and BSE images of mineral separates from nepheline syenite were obtained at the Department of Petrology and Geochemistry, Eötvös Loránd University, Budapest, Hungary using an AMRAY 1830 SEM equipped with GATAN MiniCL (3 nA, 10 kV setup). Imaging of crystals separated from syenite was carried out at the Department of Geosciences, Johann Wolfgang Goethe University, Frankfurt, Germany. In situ U–Pb geochronology was performed at the GÖOchron Laboratories, Georg-August University of Göttingen, Göttingen, Germany, using an excimer laser and a Thermo Finnigan Element2 sector field mass spectrometer.

The spot diameters were 23 and 33 µm with an ablation system of ASI Resolution 155. The method employed for analysis is described in detail by Frei and Gerdes (2009). GJ-1 reference zircon (Jackson et al., 2004) was used as "primary standard" and Plešovice zircon (Sláma et al., 2008) and 91500 zircon (Wiedenbeck et al., 1995) were measured as

secondary reference materials along with unknown zircon crystals. The MKED1 reference material (Spandler et al., 2016) was used as primary titanite standard, whereas the OLT1 (Kennedy et al., 2010) and BLS (Aleinikoff et al., 2007) were applied as secondary reference materials.

The concordia plots were constructed by IsoplotR (Vermeesch, 2018).

PETROGRAPHY OF THE DATED SAMPLES

Amphibole- and pyroxene-rich cumulate

Amphibole- and pyroxene-rich cumulate (VRG6546/b) consists of idiomorphic–hypidiomorphic cumulus amphibole (Fig. 3A) with variable grain size (macrocrysts ≤ 11 mm; microcrysts: 100–500 μm). Amphibole oikocrysts (larger than 10 mm) are rich in clinopyroxene, titanite, magnetite and apatite inclusions. Some of the amphiboles alter to epidote and chlorite. Clinopyroxene (≤ 16 V/V%) occurs as macrocrysts or as inclusions in amphibole oikocrysts, and often shows alteration to secondary amphibole, chlorite or epidote. Hypidiomorphic biotite occurs in small amount (1–20 V/V%). Hypidiomorphic–xenomorphic intercumulus plagioclase (≤ 12 V/V%) fills up residual space between mafic minerals. Magnetite (≤ 5 V/V%), primary titanite (≤ 3 V/V%) and apatite (≤ 5 V/V%) occur as inclusions in cumulus minerals and as intergranular crystals.

Syenite

Syenite (VRG7404, VRG7425) is phaneritic with a medium to coarse-grained, inequigranular, serial and hypidiomorphic texture. It consists of alkaline feldspar (67–81 V/V%) and plagioclase (18–26 V/V%), accompanied by muscovite (0–1 V/V%), cancrinite (0–7 V/V%) and primary accessory minerals (apatite, zircon and titanite) (0–4 V/V%) (Fig. 3B). Mafic minerals of the groundmass occur in negligible amounts (biotite: 0–1 V/V%). Mafic components form aggregates enclosed in the syenite, comprising amphibole (4–83 V/V%), biotite (3–59 V/V%), clinopyroxene (0–7 V/V%), minor amounts of alkaline and plagioclase feldspars (1–13 and 1–10 V/V%, respectively), accessory- (apatite, zircon and titanite; 0–22 V/V%) and opaque minerals (1–14 V/V%).

Nepheline syenite

Nepheline syenite (VRG6836, VRG7546) is holocrystalline and displays an equigranular, medium to coarse-grained texture. The most common rock-forming minerals are idiomorphic nepheline (7–35 V/V%) and hypidiomorphic–xenomorphic alkaline feldspar (59–90 V/V%) (Fig. 3C). Nepheline is 5–15 mm in size, albeit it often occurs as microcrystals (~ 0.5 mm). Along cracks and fissures nepheline is replaced by cancrinite, sodalite or analcime. The amount of plagioclase is negligible (≤ 10 V/V%). The dominant mafic components are biotite (2–10 V/V%), clinopyroxene (2–7 V/V%) and amphibole (2–5 V/V%). Titanites occur in two

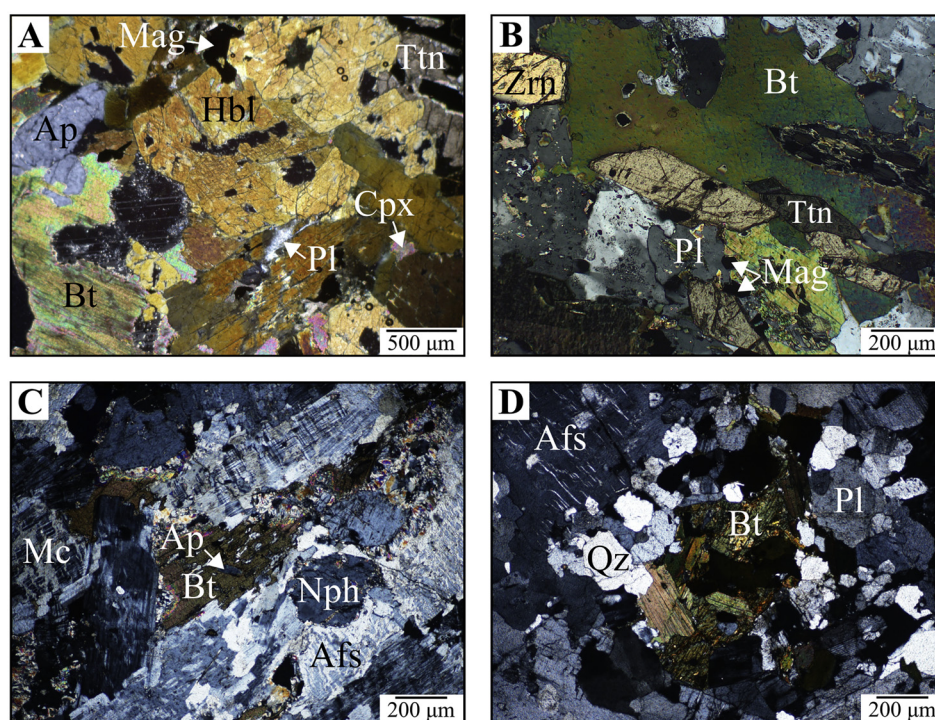


Fig. 3. Characteristic textural features of the studied rocks. (A) Cumulus amphibole and titanite with intercumulus plagioclase in amphibole- and pyroxene-rich cumulate (VRG6546/b), +N (crossed polarized light). (B) Biotite, zircon and titanite in syenite (VRG7404), +N. (C) Biotite and nepheline in nepheline syenite (VRG6836), +N. (D) Biotite aggregate in granite (VRG6831), +N. Abbreviations of rock-forming minerals are after Whitney and Evans (2010)

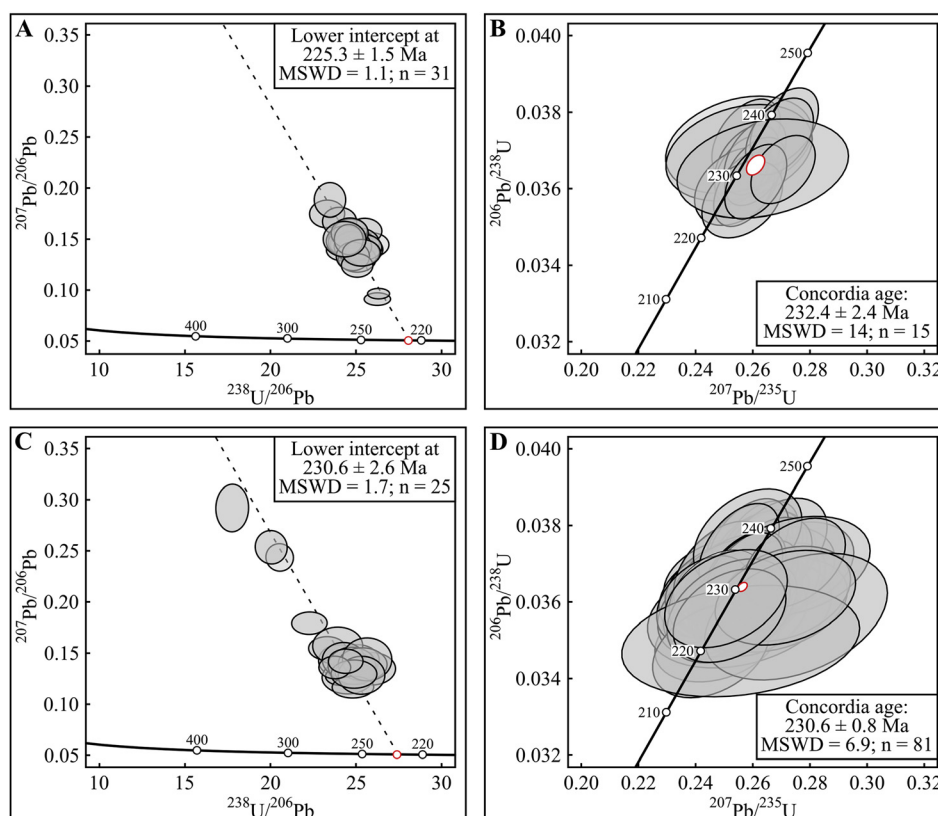


Fig. 4. Results of U-Pb geochronology. (A) Syenite U-Pb age data of titanite spots on Tera-Wasserburg concordia plot. (B) Concordant zircon U-Pb isotopic data of syenite on Wetherill plot with concordia age. (C) Nepheline syenite U-Pb age data of titanite spots on Tera-Wasserburg concordia plot. (D) Concordant zircon U-Pb isotopic data of nepheline syenite on Wetherill plot with concordia age

generations: 0.1–0.3 and 2.1–2.5 mm in size. Additional magmatic accessory phases are apatite, zircon, magnetite and ilmenite (3–5 V/V%).

Granite

Granite (VRG6827, VRG6831, VRG6853) is phaneritic and inequigranular. It is composed of alkaline feldspar (24–45 V/V %), plagioclase (21–35 V/V%) and quartz (17–31 V/V%) (Fig. 3D). Microcline is often poikilitic and encloses plagioclase, quartz and biotite. Two generations of plagioclases can be recognized: (a) megacrystalline, zoned and sericitic; (b) smaller sized and myrmekitic. Mafic constituents (3–25 V/V %) are represented by biotite and amphibole. Altered amphibole is often accompanied by opaque minerals, biotite and epidote. Secondary rutile and titanite aggregates occur along the cleavage faces of altered biotite. Zircon, titanite, apatite and magnetite are the most common primary accessory minerals.

RESULTS

K/Ar geochronology

Results of K/Ar age dating can be found in Fig. 5 and Table 2. Amphibole of amphibole- and pyroxene-rich cumulate yielded a K/Ar mean age of 238.6 ± 8.9 Ma. An age of 216.0 ± 8.1 Ma was determined for amphibole of

nepheline syenite. K/Ar ages of biotite from granite are 201.4 ± 7.6 and 198.3 ± 7.5 Ma. Amphibole of granite gave K/Ar mean ages of 197.3 ± 7.4 and 196.3 ± 7.4 Ma.

U-Pb geochronology

The textural homogeneity of the studied titanite and zircon crystals was inspected using CL and BSE images. The ideal spots for analyses were selected based on these images, in order to avoid crystal parts containing inclusions, different texture or cracks. CL images usually show normal magmatic zoning of the examined titanite and zircon grains. Older or texturally disparate crystal domains were only observed in the case of zircon samples.

Syenite

In-situ U-Pb dating was performed on 15 rim and 16 core domains of titanite crystals. The different growth zones did not yield distinguishable ages within uncertainty. The amount of non-radiogenic ^{206}Pb isotope is high; thus, one can consider the matrix-corrected lower intercept age of 225.3 ± 1.5 Ma with an MSWD value of 1.1 on the Tera-Wasserburg diagram as a relevant datum ($n = 31$; Fig. 4A), and an interpreted main crystallization age of 225.3 ± 2.7 Ma (with 1% external uncertainties; Table 3).

In-situ U-Pb dates of 32 zircon spots on 12 crystals were measured. The obtained data were filtered according to their

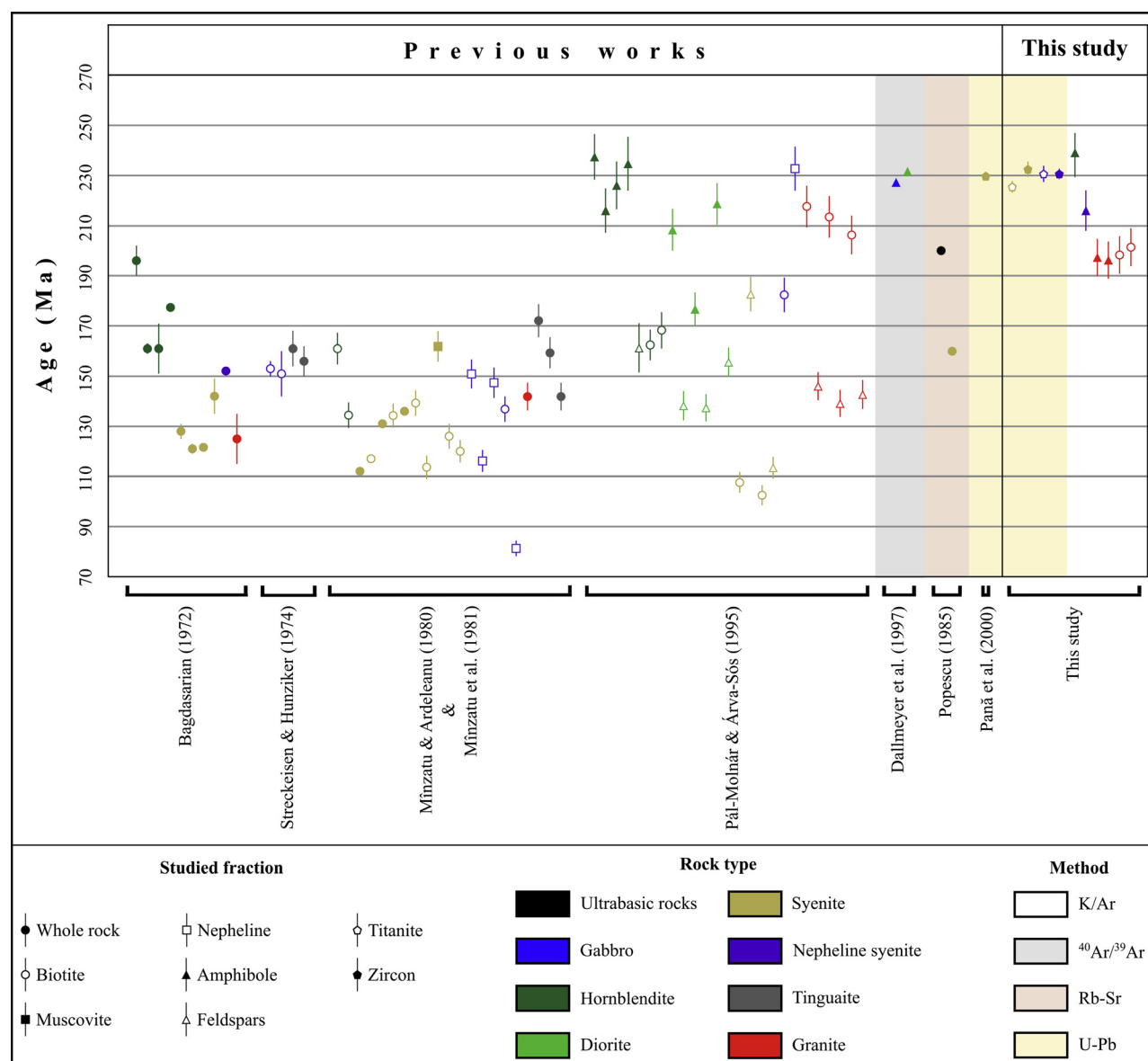


Fig. 5. Previously published results and our new geochronological data from the Ditrău Alkaline Massif

Table 2. Results of K/Ar age dating

Sample	Rock type	Locality and GPS coordinates	Studied fraction	K-content (%)	$^{40}\text{Ar}_{\text{rad/g}}$ (ncm^3/g)	$^{40}\text{Ar}_{\text{rad}}$ (%)	Age (Ma)
VRG6546/b	Amphibole- and pyroxene-rich cumulate	Jolotca, Tarnița de Sus creek 46.87454, 25.49871	amphibole	1.16	$1.15 \cdot 10^{-5}$	78.1	238.6 ± 8.9
VRG6836	Nepheline syenite	Jolotca, Fagului Plat creek 46.86841, 25.55315	amphibole	1.62	$1.4450 \cdot 10^{-5}$	94.8	216.0 ± 8.1
VRG6827	Granite	Jolotca, Turcului creek 46.8706, 25.55029	amphibole	3.41	$2.7641 \cdot 10^{-5}$	93.6	197.3 ± 7.4
VRG6831	Granite	Jolotca, Turcului creek 46.88141, 25.55258	amphibole	1.33	$1.0719 \cdot 10^{-5}$	87.7	196.3 ± 7.4
VRG6853	Granite	Jolotca, Creanga Mare creek 46.8743, 25.59169	biotite	3.46	$2.8194 \cdot 10^{-5}$	92.4	198.3 ± 7.5
			biotite	4.04	$3.3468 \cdot 10^{-5}$	95	201.4 ± 7.6

Table 3. Summary of U–Pb titanite and zircon ages of the studied syenite and nepheline syenite samples from the Ditrău Alkaline Massif

Sample	Rock type	Locality and GPS coordinates	Studied fraction	Number of measured data/ concordant data	Lower intercept age (Ma)	MSWD	Concordia age (number of dates included)	MSWD	Interpreted main crystallisation age (Ma) with uncertainty (including 1% external uncertainties)
VRG7404	Syenite	Teasc creek 46.88086, 25.51715	titanite	30/0	225.3 ± 1.5	1.1	n.d.	n.d.	225.3 ± 2.7
VRG7546	Nepheline syenite	Teasc creek 46.88461, 25.5132	titanite	25/0	230.6 ± 2.6	1.5	n.d.	n.d.	230.6 ± 3.5
VRG7425	Syenite	Holoşag creek 46.87458, 25.53758	zircon	32/15	n.d.	n.d.	232.4 ± 2.4 (15)	14	232.4 ± 3.3
VRG7546	Nepheline syenite	Teasc creek 46.88461, 25.5132	zircon	105/82	n.d.	n.d.	230.6 ± 0.8 (81)	6.9	230.6 ± 2.4

discordance (<5%) and resulted in 15 concordant dates, varying between 238.1 and 226.3 Ma. The calculated concordia age is 232.4 ± 2.4 Ma that has a relatively high (14) MSWD value (overdispersion is included in the uncertainty; Vermeesch, 2018; Fig. 4B). The interpreted main zircon crystallization age is 232.4 Ma, with an uncertainty of ± 3.3 Ma (including 1% external uncertainties; Table 3).

Nepheline syenite

The analyzed titanite crystals show around 10% non-radiogenic ^{206}Pb contents; thus, one can apply the fractionation-corrected lower intercept age of 230.6 ± 2.6 Ma with an MSWD value of 1.7 on the Tera-Wasserburg diagram as a relevant datum (Fig. 4C) and an interpreted crystallization age of 230.6 ± 3.5 Ma ($n = 25$; with external uncertainties; Table 3).

In-situ U–Pb dating was performed on two grain-size fractions of zircon crystals. The obtained 105 data were filtered according to their discordance (<5%). There was no difference in age between the grain size fractions. Analyses yielded 82 concordant ages, ranging between 238.7 and 220.1 Ma. One older, xenocrystic date of 757.8 Ma was detected. The concordia age is 230.6 ± 0.8 Ma, with an MSWD of 6.9 (uncertainty includes the overdispersion of MSWD; Vermeesch, 2018; Fig. 4D). The main zircon crystallization age is 230.6 Ma, with an uncertainty of ± 2.4 Ma (including 1% external uncertainties; Table 3).

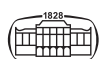
DISCUSSION

According to our field structural and petrographic observations, the following inferences can be drawn: (a) based on petrographic and genetic aspects, cumulate rocks (e.g.,

hornblende, olivine-rich cumulate, amphibole- and pyroxene-rich cumulate, amphibole-rich cumulate), gabbro and diorite should not be classified into different rock-complexes (e.g., Anastasiu and Constantinescu, 1979; Zólya and Zólya, 1985, 1986; Pál-Molnár, 1988). It can be noticed that these rock types occur adjacently (Fig. 1B) with either abrupt or gradual transition to each other. After Pál-Molnár (2000), the rock association of this structurally and tectonically complex lithostratigraphic unit is referred to as the Tarnița Complex. Detailed petrogenetic interpretation of this unit can be found in Pál-Molnár et al. (2015b) and Heincz et al. (2018); (b) the gradual transition between diorite, monzodiorite, monzonite and syenite is difficult to trace in the field; (c) transition between syenite, quartz syenite and granite can also be continuous; (d) different-sized metamorphic xenoliths occur in syenite and granite; (e) rocks of the Tarnița Complex, diorite-syenite and syenite-granite transition zones are cross-cut by nepheline syenite; (f) syenite intruded into the Tarnița Complex; (g) nepheline syenite and rocks of (a)–(f) are cross-cut by tinguaitite dykes; (h) lamprophyre dykes intersect all other rock types of the massif.

Geochronological data

Comparing the results of previous work with our new K/Ar and U–Pb data (Tables 1–3) the diversity of obtained ages, ranging between 238.6 ± 8.9 Ma and 81.3 ± 3.1 (Fig. 5) can be observed. This phenomenon can be explained by the fact that different authors performed K/Ar analyses on various minerals with different closure temperature; however, interpretation of these data should be carried out with caution. Bagdasarian (1972), Streckeisen and Hunziker (1974), Minzatu and Ardeleanu (1980), as well as Minzatu et al. (1981) determined whole rock ages. The results of these



analyses are mostly mixed ages, due to the different closure temperature and resistance of the minerals. K/Ar data of biotite and feldspars – considering the low closure temperature of these phases – yield the age of postmagmatic events. This means that the ages obtained from minerals with higher closure temperature for the K/Ar decay system [i.e., amphibole: 510 ± 25 °C (Harrison, 1981); Pál-Molnár and Árvai-Sós, 1995; Dallmeyer et al., 1997] and the U–Pb ages of titanite and zircon (Pană et al., 2000; this study) could provide the most relevant information about the timing of the magmatic events. The K/Ar age of amphiboles yield reliable information solely when the solidus of the crystallizing magma and the closure temperature of amphibole are comparable. It must be noticed that the amphibole of this study dated by K/Ar method originates from a cumulate rock that – based on previous thermobarometric calculations of Almási et al. (2015) and Pál-Molnár et al. (2015b) – crystallized at considerably higher temperatures (900–1050 °C) than the typical closure temperature of amphibole. Hence, the K/Ar age of the studied amphibole sample displays the minimum crystallization age of the amphibole- and pyroxene-rich cumulate rock. The analyzed titanite and zircon crystallization dates of syenite and nepheline syenite samples are mostly equal within uncertainty and are concordant with the 229.6 ± 1.7 – 1.2 Ma ID-TIMS age of the zircon crystals from a syenite sample published by Pană et al. (2000). This is also in age-agreement with the amphibole data of hornblende determined by Pál-Molnár and Árvai-Sós (1995) and with amphibole data of gabbro and diorite analyzed by Dallmeyer et al. (1997).

The emplacement sequence of the different rock types of the massif – considering field occurrences and overlapping age data – is as follows: cumulate rocks, diorite, monzodiorite, monzonite, syenite, quartz syenite, granite, nepheline syenite, tinguaita, lamprophyre.

Taking into account all age data from the examined rock types in this study, they reveal a slightly broad age span, from 238.6 ± 8.9 Ma (amphibole from cumulate rock by K/Ar method) to 196.3 ± 7.4 Ma (amphibole from granite by K/Ar method). Nevertheless, the younger dates are possibly affected by post-magmatic fluids, similarly to those younger ages from previous studies using K/Ar and Rb–Sr methods. Therefore, the lower limit of the magmatic event age is questionable, since both the archive data and the new K/Ar ages exhibit wide scattering. The upper limit is also ambiguous, as the highest age-value (238.6 ± 8.9 Ma of amphibole from amphibole- and pyroxene-rich cumulate; this study) was determined by the K/Ar method and shows a significant error, overlapping the U–Pb ages.

According to these, it can be concluded that the igneous event age could be most plausible between 238.6 ± 8.9 Ma (amphibole from amphibole- and pyroxene-rich cumulate; this study) and 225.3 ± 2.7 Ma (titanite from syenite; this study), keeping in mind that the most significant U–Pb data scatter around ~ 230 Ma.

Using the methodology we have so far, there is no resolvable age difference between the early emplaced cumulate rocks and the late nepheline syenite.

These data contradict the age-range of the multi-stage evolution theory of the DAM proposed by Morogan et al. (2000) and disprove the age-range of the two and multi-stage formation hypothesis of Pál-Molnár and Árvai-Sós (1995), Kräutner and Bindea (1998), as well as of Pál-Molnár (2000, 2008).

Palinspastic reconstruction

Based on previous geochemical results (e.g., Morogan et al., 2000; Pál-Molnár 2000, 2010b; Batki et al., 2014; Pál-Molnár et al., 2015b) the DAM was emplaced in an intra-plate, rift-related tectonic environment. Considering the age- and geochemical data, the formation of the massif can be attributed to the evolution of Western-Tethys. Several authors (e.g., Kozur, 1991; Stampfli and Borel, 2002, 2004; Hoeck et al., 2009; Pană, 2010) have made attempts to interpret the rifting and subducting events of the separate oceanic basins of Tethys. Contrasting palinspastic reconstructions have been developed due to the complex structure and tectonic evolution of the area. The formation of the Alps and Carpathians is coherent with the evolution of Meliata-Maliac/Vardar Oceans (Stampfli and Borel, 2002).

According to Stampfli and Borel (2002), the Neotethys started to open in the Late Carboniferous–Early Permian period. This process initiated the drifting of the Cimmerian Block from Pangea and the subduction of Paleotethys in the Middle–Late Triassic period. Slab roll-back of Paleotethys resulted in the formation of back-arc basins along the southern Eurasian margin. Some of these basins evolved into an oceanic basin. Several back-arc basins (e.g., Karakaya, Küre) closed due to the Cimmerian collision in the Jurassic. The Meliata, Maliac and Pindos oceanic branches remained open until the Late Jurassic. Their subduction initiated the opening of further back-arc basins (e.g., Vardar). Subduction of the Küre Ocean was accompanied by the closure of the Meliata-Maliac Ocean in the Late Triassic–Early Jurassic (Stampfli and Borel, 2002).

Kozur (1991) made two Middle–Late Triassic palinspastic reconstructions for the Eastern Carpathians: (a) the postulated Central Dinaric Ocean was situated between the High Karst Zone and the Lim/Bosnian Zone. The two branches of this ocean were the Hallstatt and Meliata Oceans. The Transylvanian–Pieniny Ocean occupied an adjacent but separate basin; (b) according to the second hypothesis of Kozur (1991), a triple junction was formed in the Eastern Carpathians. One of its branches, the Pieniny Ocean, opened up during the Early Anisian, whereas Meliata evolved in the Middle Anisian. The Transylvanian Ocean extended through the Strandzha Zone to the Pontides. Based on Kozur (1991), the Meliata Ocean closed in the Late Jurassic (Oxfordian); its remnants are represented by obducted nappes enclosing ophiolites.

Middle–Late Triassic ophiolite breccias and olistholites occur in the Late Barremian–Early Albian Wildflysch of Rarău, Hăghimaş and Perşani Mountains (Eastern Carpathians). Hoeck et al. (2009) proposed that these rocks are remnants of a subducted oceanic crust, formerly located

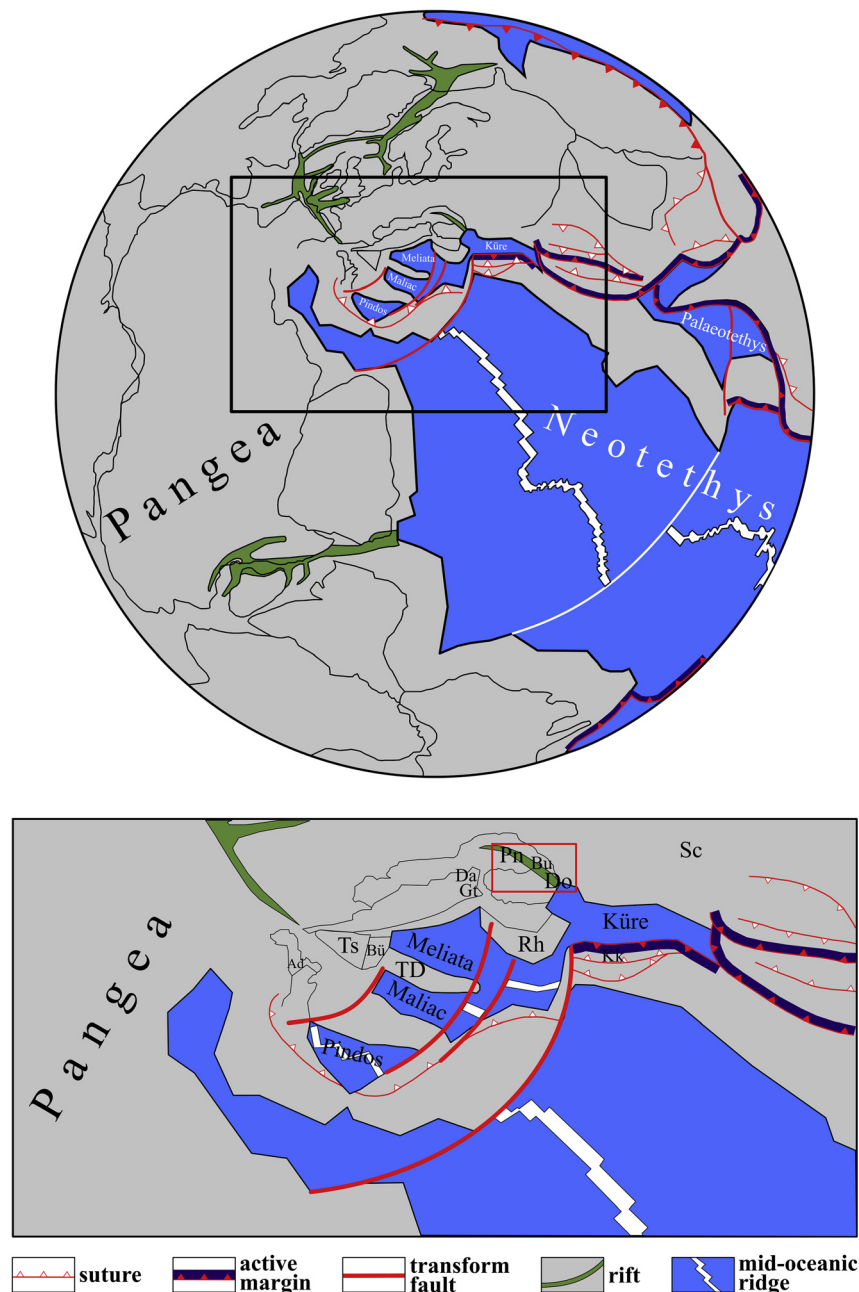


Fig. 6. Middle–Late Triassic palinspastic reconstruction (modified after Stampfli and Borel, 2002). Legend: Ad – Adria s. str.; Bu – Bucovinian; Bü – Bükk; Da – Dacides; Do – Dobrogea; Gt – Getic; Kk – Karakaya forearc; Pn – Pienniny rift; Rh – Rhodope; Sc – Scythian platform; TD – Trans-Danubian; Ts – Tisia

between the Bucovinian, Infrabucovinian and Northern Apuseni continental panels. The emplacement of the DAM can be attributed to the opening of the oceanic basin. Analogous Middle Triassic intrusions occur in the Southern Alps (Castellarin et al., 1982) and Dinarides (Pamić, 1984). The opening of the Vardar Ocean induced the subduction of the oceanic branch beneath the Northern Apuseni and Infrabucovinian units. The ocean closed in the Late Triassic–Early Jurassic (Hoeck et al., 2009).

Pană (2010) did not agree with the hypothesis of Hoeck et al. (2009), considering (a) that the entire ophiolite suite is not represented, (b) that the studied rocks are located in an

intra-continental tectonic setting and (c) that the reported age data are not precise enough. Pană (2010) questioned the credibility of the palinspastic reconstruction of Hoeck et al. (2009). According to Hoeck et al. (2009), the Northern Apuseni block was located north of the Meliata Ocean, albeit Triassic sediments and volcanic rocks of the Northern Apuseni Mountains can be correlated with rocks formed south of the Meliata Ocean (Channell and Kozur, 1997). In the absence of geologic evidence, Pană (2010) argued the hypothesis that the oceanic crust subducted beneath the Northern Apuseni and Infrabucovinian continental domains in the Late Triassic–Early Jurassic.

Geochronological data are in correspondence with the reviewed palinspastic reconstructions and petrogenesis of the DAM. Considering this information, the Ditrău Alkaline Massif was formed in an intra-plate, rift-related extensional tectonic setting at the southwestern margin of the East European Craton (Fig. 6; the postulated area of emplacement is marked by a red rectangle) during the Middle–Late Triassic.

CONCLUDING REMARKS

Previous, mostly K/Ar geochronological data of the Ditrău Alkaline Massif have been supplemented and refined by new, more precise K/Ar and U–Pb age data. U–Pb geochronology of accessory minerals is the most reliable method to determine the age of magmatic processes, while postmagmatic thermal events can be traced by the K/Ar decay system.

A K/Ar age of 238.6 ± 8.9 Ma was obtained for amphibole of the amphibole- and pyroxene-rich cumulate. Based on in-situ U–Pb dating, titanite and zircon from syenite were formed at 225.3 ± 2.7 Ma and 232.4 ± 3.3 Ma, respectively. Nepheline syenite yielded a K/Ar age of 216.0 ± 8.1 Ma, as well as U–Pb titanite and zircon age of 230.6 ± 3.5 and 230.6 ± 2.4 Ma, respectively. K/Ar age of biotite from granite ranges from 201.4 ± 7.6 to 196.3 ± 7.4 Ma. Considering new and previous (post-1990) K/Ar and U–Pb data, the crystallization of the massif took place between 238.6 ± 8.9 and 225.3 ± 2.7 Ma (noting that the most relevant U–Pb ages scatter around ~ 230 Ma).

Age data and tectonic analogies suggest a short magmatic span (Middle–Late Triassic, Ladinian–Norian) of the Ditrău Alkaline Massif. Magmatism could be associated with an intra-plate, rift-related extensional tectonic setting at the southwestern margin of the East European Craton.

ACKNOWLEDGEMENTS

The authors are grateful to the staff of ‘Vulcano’ Petrology and Geochemistry Research Group, Department of Mineralogy, Geochemistry and Petrology, University of Szeged, Szeged, Hungary and to the technician of the MTA-ELTE Volcanology Research Group. Axel Gerdes of Goethe University, Frankfurt, Germany is gratefully acknowledged for his assistance with preliminary U–Pb analyses. A thorough review, helpful comments and valuable suggestions of Zsolt Benkó (Institute for Nuclear Research, Hungarian Academy of Sciences, Debrecen, Hungary) and of an anonymous reviewer are highly appreciated. Gábor Dobosi is gratefully acknowledged for his editorial work on the manuscript.

REFERENCES

Aleinikoff, J.N., Wintsch, R.P., Tollo, R.P., Unruh, D.M., Fanning, C.M., and Schmitz, M.D. (2007). Ages and origins of rocks of

the Killingworth dome, south-central Connecticut: implications for the tectonic evolution of southern New England. *American Journal of Science*, 307: 63–118.

Almási, E.E., Batki, A., and Kiss, B. (2015). Amfibolok petrogenezis-jelentősége a Ditrői alkáli masszívum ultramafikus kumulátumközeteiben. *Földtani Közlemények*, 145(3): 229–246.

Anastasiu, N. and Constantinescu, E. (1979). *Structura și petrogeneza masivului alcalin de la Ditrău*, Raport geologic final. Archiva IPEG Harghita, Miercurea-Ciuc, manuscript.

Bagdasarjan, G.P. (1972). Despre vârsta absolută a unor roci eruptive și metamorfice din masivul Ditrău și Munții Banatului din România. *Studii și Cercetări Geologie, Geofizică, Geografie, Seria Geologie*, 17(1): 13–21.

Balintoni, I. (1997). *Geotectonica terenurilor metamorfice din România*. Cluj Napoca, Carpatica, pp. 176.

Balintoni, I. and Balica, C. (2013). Carpathian peri-Gondwanan terranes in the East Carpathians (Romania): a testimony of an Ordovician, North-African orogeny. *Gondwana Research*, 23(3): 1053–1070.

Balintoni, I., Balica, C., Ducea, H., and Horst-Peter, H. (2014). Peri-Gondwanan terranes in the Romanian Carpathians: a review of their spatial distribution, origin, provenance, and evolution. *Geoscience Frontiers*, 5(3): 395–411.

Balintoni, I., Gheuca, I., and Vodă, Al. (1983). Pânze de încălecare Alpine și Hercinice din zona sudică și centrală a Zonei Cristaline Mezozoice din Carpații Orientali. (Alpine and Hercynian overthrust nappes from central and southern areas of the East Carpathians Crystalline Mesozoic Zone). *Anuarul Institutului de Geologie și Geofizică al României*, 60: 15–22.

Balogh, K. (1985). K/Ar dating of Neogene volcanic activity in Hungary: experimental technique, experiences and methods of chronological studies. *Atomki Közlemények*, 27(3): 277–288.

Batki, A., Pál-Molnár, E., and Bárdossy, A. (2004). Occurrence and petrology of lamprophyres from the northern part of the Ditrău Alkaline Massif, Eastern Carpathians, Romania. *Acta Mineralogica-Petrographica*, 45(2): 21–28.

Batki, A., Pál-Molnár, E., Dobosi, G., and Skelton, A. (2014). Petrogenetic significance of ocellar camptonite dykes in the Ditrău Alkaline Massif, Romania. *Lithos*, 200–201: 181–196.

Batki, A., Pál-Molnár, E., Jankovics, M.É., Kerr, A.C., Kiss, B., Markl, G., Heincz, A., and Harangi, Sz. (2018). Insights into the evolution of an alkaline magmatic system: An in situ trace element study of clinopyroxenes from the Ditrău Alkaline Massif, Romania. *Lithos*, 300–301: 51–71.

Castellarin, A., Lucchini, F., Rossi, P.L., Sartori, R., Simboli, G., and Sommariva, E. (1982). Note geologiche sulle intrusioni di Predazzo e dei M. Manzon. In: Castellarin, A. and Vai, G.B. (Eds.), *Guida alla geologia del Sudalpino Centro-Orientale*. Bologna: Guide Geol. Reg. Società Geologica Italiana, pp. 211–219.

Channell, J.E.T. and Kozur, H.W. (1997). How many oceans? Meliata, Vardar and Pindos oceans in Mesozoic Alpine paleogeography. *Geology*, 25: 183–186.

Codarcea, Al., Codarcea, D.M., and Ianovici, V. (1957). Structura geologică a masivului de roci alcaline de la Ditrău. *Buletin Științific R. P. R. Geologie, Geografie*, 2(3–4): 385–446.

Codarcea, Al., Ianovici, V., Iova, I., Lupan, S., and Papacostea, C. (1958). Elemente rare în masivul de la Ditrău. *Com. Acad. R. P. R.*, 8(3): 321–326.



- Cohen, K.M., Finney, S.C., Gibbard, P.L., and Fan, J.-X. (2013, updated). The ICS International Chronostratigraphic Chart. *Episodes*, 36: 199–204.
- Dallmeyer, D.R., Kräutner, H.G., and Neubauer, F. (1997). Middle-late Triassic $^{40}\text{Ar}/^{39}\text{Ar}$ hornblende ages for early intrusions within the Ditrău alkaline massif, Rumania: implications for Alpine rifting in the Carpathian orogen. *Geologica Carpathica*, 48: 347–352.
- Fall, A., Bodnar, R.J., Szabó, Cs., and Pál-Molnár, E. (2007). Fluid evolution in the nepheline syenites of the Ditrău Alkaline Massif, Transylvania, Romania. *Lithos*, 95: 331–345.
- Frei, D. and Gerdes, A. (2009). Precise and accurate in situ U-Pb dating of zircon with high sample throughput by automated LASF-ICP-MS. *Chemical Geology*, 261(3–4): 261–270.
- Harrison, T.M. (1981). Diffusion of ^{40}Ar in hornblende. *Contributions to Mineralogy and Petrology*, 78: 324–331.
- Heincz, A., Pál-Molnár, E., Kiss, B., Batki, A., Almási, E.E., and Kiri, L. (2018). Nyílt rendszerű magmás folyamatok: magmaakeveredés, kristálycsere, kumulátum recirkuláció nyomai a Ditrói Alkáli Masszívumban (Orotva, Románia). *Földtani Közöny*, 148(2): 125–142.
- Hoek, V., Ionescu, C., Balintoni, I., and Koller, F. (2009). The Eastern Carpathians “ophiolites” (Romania): remnants of a triassic ocean. *Lithos*, 108: 151–171.
- Jackson, S.E., Pearson, N.J., Griffin, W.L., and Belousova, E.A. (2004). The application of laser ablation-inductively coupled plasma-mass spectrometry to in situ U–Pb zircon geochronology. *Chemical Geology*, 211: 47–69.
- Kennedy, A.K., Kamo, S.L., Nasdala, L., and Timms, N.E. (2010). Grenville skarn titanite: potential reference material for SIMS U–Th–Pb analysis. *Canadian Mineralogist*, 48: 1423–1443.
- Koch, A. (1876). *Erdély keleti részének némely geológiai viszonyai*, Előadás, Kolozsvári orv. term. tud. társulat 1876. évi értesítője.
- Koch, A. (1879). A ditrói syenitörmzs közzetani és hegyszerkezeti viszonyairól. *Magyar Tudományos Akadémia, Értekezések*, 9(2).
- Kozur, H. (1991). The evolution of the Meliata-Hallstatt ocean and its significance for the early evolution of the Eastern Alps and Western Carpathians. *Palaeogeography, Palaeoclimatology, Palaeoecology*, 87: 109–135.
- Kräutner, H.G. (1996–1997). Alpine and pre-Alpine terranes in the Romanian Carpathians and Apuseni Mountains. In: Papanikolaou, D. (Ed.), *Terrane maps and terrane descriptions. IGCP Project No. 276. Annales Geologiques des Pays Helleniques*, Athens, pp. 331–400.
- Kräutner, H.G. and Bindea, G. (1995). The Ditrău alkaline intrusive complex and its geological environment. *Romanian Journal of Mineralogy*, 77(3): 1–44.
- Kräutner, H.G. and Bindea, G. (1998). Timing of the Ditrău alkaline intrusive complex (Eastern Carpathians, Romania). *Slovak Geological Magazine*, 4: 213–221.
- Kräutner, H.G., Kräutner, Fl., Tănăsescu, A., and Neacșu, V. (1976). Interpretation des âges radiométriques K–Ar pour les roches métamorphiques régénérées. Un exemple – les Carpates Orientales. *Analele Institutului de Geologie și*, 50: 167–229.
- Lilienbach, L. (1833). Journal d’un voyage géologique fait en travers toute la chaîne des Carpathes, en Bucovine, en Transylvanie et dans le Marmarosch. *Mémoires de la Société géologique de France*, 1: 237–316.
- Mînzatu, S. and Ardeleanu, P. (1980). *Detailed radiometric research in the Ditrău massif (in Romanian, manuscript)*, Arch. IPEG “Harghita” (Miercurea-Ciuc).
- Mînzatu, S., Văjdea, E., Romanescu, O., and Iosipenco, N. (1981). *K–Ar ages of the Ditrău massif (in Romanian, manuscript)*, Arch. IGG (Bucuresti).
- Morogan, V., Upton, B.G.J., and Fitton, J.G. (2000). The petrology of the Ditrău alkaline complex, Eastern Carpathians. *Mineralogy and Petrology*, 69: 227–265.
- Odin, G.S and 35 Collaborators (1982). Interlaboratory standards for dating purposes. In: Odin, G.S. (Ed.), *Numerical dating in stratigraphy*. Wiley and Sons, Chichester, pp. 123–149.
- Pál-Molnár, E. (1988). *Studiul mineralogic și petrologic al complexului Jolotca din masivul alcalin de la Ditrău, cu privire specială asupra mineralelor purtătoare de fier*, MSc-thesis, Babeș-Bolyai University, Cluj-Napoca, Romania, p. 127.
- Pál-Molnár, E. (1994a). *A Ditrói szienitmasszívum kialakulása a földtani megismerés tükrében (Formation of the Ditrău Syenite Massif in view of geological aspects)*, A Magyar Tudományos Akadémia Szegedi Akadémiai Bizottságának Kiadványai, Szeged, p. 85.
- Pál-Molnár, E. (1994b). *Adalékok a Ditrói szienitmasszívum szerkezeti és közzetani ismeretéhez (Contributions on structural and petrological knowledge of Ditró syenite massif)*. MTA SzAB Competition, manuscript.
- Pál-Molnár, E. (2000). *Hornblendites and diorites of the Ditró Syenite Massif*. Department of Mineralogy, Geochemistry and Petrology, University of Szeged, Szeged, p. 172.
- Pál-Molnár, E. (2008). Mezozoos alkáli magmatizmus a Kárpát régióban: a Ditrói Alkáli Masszívum Petrogenezise. *OTKA zárójelentés*, p. 80.
- Pál-Molnár, E. (2010a). Rock-forming minerals of the Ditrău Alkaline Massif. In: Szakáll, S. and Kristály, F. (Eds.), *Mineralogy of Székelyland, Eastern Transylvania, Romania. Csík County Nature and Conservations Society, Sfântu Gheorghe–Miercurea-Ciuc–Târgu Mureș*, pp. 63–88.
- Pál-Molnár, E. (2010b). Geology of Székelyland. In: Szakáll, S. and Kristály, F. (Eds.), *Mineralogy of Székelyland, Eastern Transylvania, Romania. Csík County Nature and Conservations Society, Sfântu Gheorghe–Miercurea-Ciuc–Târgu Mureș*, pp. 33–43.
- Pál-Molnár, E. and Árva-Sós, E. (1995). K/Ar radiometric dating on rocks from the northern part of the Ditró syenite massif and its petrogenetic implications. *Acta Mineralogica-Petrographica, Szeged*, 36: 101–116.
- Pál-Molnár, E., Batki, A., Ódri, Á., Kiss, B., and Almási, E.E. (2015a). Geochemical implications of the magmatic origin of granitic rocks from the Ditrău Alkaline Massif (Eastern Carpathians, Romania). *Geologia Croatica*, 68(1): 51–66.
- Pál-Molnár, E., Batki, A., Almási, E.E., Kiss, B., Upton, B.G.J., Markl, G., Odling, N., and Harangi, Sz. (2015b). Origin of mafic and ultramafic cumulates from the Ditrău Alkaline Massif, Romania. *Lithos*, 239: 1–18.
- Pamić, J. (1984). Triassic magmatism of the Dinarides in Yugoslavia. *Tectonophysics*, 109: 273–307.
- Pană, D. (2010). Discussion of “The Eastern Carpathians ‘ophiolites’ (Romania) Remnants of a Triassic ocean” [*Lithos*, 108, 151–171]. *Lithos*, 115: 279–282.
- Pană, D., Balintoni, I., and Heaman, L. (2000). Precise U–Pb zircon dating of the Syenite Phase from the Ditrău Alkaline Igneous

- Complex. *Studia Universitatis Babeş-Bolyai, Geologia*, 45(1): 79–90.
- Popescu, G. (1985). *Rb–Sr geochronological data on rocks of the Ditrau Massif*, Arh. GEOLEX “Harghita”, Miercurea-Ciuc, Manuscript.
- Reinhardt, M. (1911). Sur l’âge de l’intrusion du syénite néphélinique de Ditró, Transylvanie. *Comptes -rendus de l’Institut Géologique de Roumanie*, 2: 116.
- Săndulescu, M. (1984). *Geotectonica României*. Editura Tehnică, p. 336.
- Sláma, J., Košler, J., Condon, D.J., Crowley, J.L., Gerdes, A., Hancher, J.M., Horstwood, M.S.A., Morris, G.A., Nasdala, L., Norberg, N., et al. (2008). Plešovice zircon – A new natural reference material for U–Pb dating and Hf isotopic microanalyses. *Chemical Geology*, 249(1–2): 1–35.
- Spandler, C., Hammerli, J., Sha, P., Hilbert-Wolf, H., Hu, Y., Roberts, E., and Schmitz, M. (2016). MKED1: A new titanite standard for in situ analysis of Sm–Nd isotopes and U–Pb geochronology. *Chemical Geology*, 425: 110–126.
- Stampfli, G.M. and Borel, G.D. (2002). A plate tectonic model for the Paleozoic and Mesozoic constrained by dynamic plate boundaries and restored synthetic oceanic isochrons. *Earth and Planetary Science Letters*, 196: 17–33.
- Stampfli, G.M. and Borel, G.D. (2004). The TRANSMED Transects in space and time: constraints on the paleotectonic Evolution of the Mediterranean domain. In: Cavazza, W., Roure, F., Spakman, W., Stampfli, G.M., and Ziegler, P.A. (Eds.), *The TRANSMED Atlas. The Mediterranean Region from Crust to mantle*. Springer, Berlin, Heidelberg, pp. 53–90.
- Streckeisen, A. (1938). Das Nephelinsyenit-Massiv von Ditrau in Rumänien als Beispiel einer kombinierten Differentiation und Assimilation. *Verhandlungen der Schweizerische Naturforschende Gesellschaft*, pp. 159–161.
- Streckeisen, A. (1952). Das Nephelinsyenit-Massiv von Ditrau (Siebenbürgen), I. Teil. *Schweizerische Mineralogische und Petrographische Mitteilungen*, 32: 251–309.
- Streckeisen, A. (1954). Das Nephelinsyenit-Massiv von Ditrau (Siebenbürgen), II. Teil. *Schweizerische Mineralogische und Petrographische Mitteilungen*, 34: 336–409.
- Streckeisen, A. (1960). On the structure and origin of the Nephelinsyenite Complex of Ditrau (Transylvania, Roumania). *Rep. 21th IGC*, 13: 228–238.
- Streckeisen, A. and Hunziker, I.C. (1974). On the origin of the Nephelinsyenit Massif of Ditró (Transylvania, Romania). *Schweizerische Mineralogische und Petrographische Mitteilungen*, 54: 59–77.
- Vermeesch, P. (2018). IsoplotR: a free and open toolbox for geochronology. *Geoscience Frontiers*, 9: 1479–1493.
- Vodă, A. and Balintoni, I. (1994). Corelari lithostratigrafice în cristalinul Carpaţilor Orientali. *Studia Universitatis Babeş-Bolyai, Geologia*, 39: 61–66.
- Whitney, D.L. and Evans, B.W. (2010). Abbreviations for names of rock-forming minerals. *American Mineralogist*, 95: 185–187.
- Wiedenbeck, M., Allé, P., Corfu, F., Griffin, W.L., Meier, M., Oberli, F., von Quadt, A., Roddick, J.C., and Spiegel, W. (1995). Three natural zircon standards for U–Th–Pb, Lu–Hf trace element and REE analyses. *Geostandards Newsletter*, 19: 1–23.
- Zincenco, D. (1991). *The Ditrau alkaline massif: Contribution of Rb–Sr and K–Ar data to the petrology and timing of the massif (in Romanian, manuscript)*, Arch. Soc. Prosp., Bucureşti.
- Zincenco, D., Petrescu, M., Popescu, C., Prodănescu, I., and Zincenco, C. (1994). *Age and petrology of the Ditrau massif: Rocks of the enveloping facies*, Arh. Soc. Prosp., Bucureşti, Manuscript.
- Zólya, L. and Zólya, É.G. (1985). A geological study based on geological mapping carried out in 1:5000 scale from the area of the Putna Intunecoasa spring (in Romanian), Doc. Dept. of IPEG “Harghita”, Miercurea-Ciuc, manuscript.
- Zólya, L. and Zólya, É.G. (1986). A geological study based on geological mapping carried out in 1:5000 scale from the area of the Tilalmas-Halaság spring (in Romanian), Doc. Dept. of IPEG “Harghita”, Miercurea-Ciuc, manuscript.

APPENDICES

Appendix A. Results of U–Pb dating of titanites and zircons from syenite

Rock Nr.	Spot Nr.	Studied fraction	Isotopic data									Ages						RDC age		
			U (ppm)	Pb (ppm)	²⁰⁷ Pb/ ²³⁵ U	±1σ (%)	²⁰⁶ Pb/ ²³⁸ U	±1σ (%)	rho	²⁰⁷ Pb/ ²⁰⁶ Pb	±1σ (%)	²⁰⁷ Pb/ ²³⁵ U	±2σ (Ma)	²⁰⁶ Pb/ ²³⁸ U	±2σ (Ma)	²⁰⁷ Pb/ ²⁰⁶ Pb	±2σ (Ma)	Disc. (%)	²⁰⁶ Pb/ ²³⁸ U	±2σ (Ma)
VRG7404	136	titanite	23	135	0.72685	3.7	0.03653	1.6	0.42	0.14433	3.4	554.7	32.0	231.3	7.1	2,279.8	58.4	58.3	n.d.	n.d.
	137	(core)	25	110	0.75060	3.5	0.03912	1.6	0.45	0.13916	3.1	568.6	30.6	247.4	7.6	2,216.9	54.5	56.5	n.d.	n.d.
	138		24	134	0.73909	4.4	0.03820	1.5	0.35	0.14033	4.1	561.9	38.0	241.7	7.1	2,231.3	71.1	57.0	n.d.	n.d.
	139		23	118	0.79848	3.9	0.03866	1.8	0.45	0.14982	3.5	596.0	35.6	244.5	8.5	2,343.9	60.2	59.0	n.d.	n.d.
	143		23	118	0.77044	3.8	0.03878	1.4	0.37	0.14408	3.6	580.0	34.3	245.3	6.9	2,276.9	61.9	57.7	n.d.	n.d.
	144		24	116	0.80808	3.6	0.03705	1.6	0.45	0.15820	3.2	601.4	33.0	234.5	7.4	2,436.6	55.1	61.0	n.d.	n.d.
	145		25	189	0.72811	3.4	0.03788	1.4	0.41	0.13939	3.1	555.4	29.4	239.7	6.6	2,219.7	54.3	56.8	n.d.	n.d.
	146		22	112	0.97697	3.6	0.04056	1.8	0.49	0.17471	3.2	692.1	36.6	256.3	8.8	2,603.3	53.2	63.0	n.d.	n.d.
	147		22	133	0.76930	4.2	0.03853	1.8	0.43	0.14482	3.8	579.4	37.0	243.7	8.5	2,285.7	65.0	57.9	n.d.	n.d.
	148		21	130	0.74806	4.7	0.03774	1.8	0.38	0.14376	4.3	567.1	41.1	238.8	8.2	2,273.1	74.9	57.9	n.d.	n.d.
	149		22	129	0.71685	4.2	0.03714	1.8	0.43	0.13998	3.8	548.8	36.3	235.1	8.3	2,227.0	66.8	57.2	n.d.	n.d.
	150		19	119	0.74282	4.3	0.03785	1.8	0.43	0.14235	3.9	564.0	37.6	239.5	8.7	2,256.1	67.5	57.5	n.d.	n.d.
	151		19	126	0.78341	3.8	0.03881	1.7	0.46	0.14641	3.4	587.4	34.1	245.4	8.3	2,304.5	58.2	58.2	n.d.	n.d.
	152		21	142	0.75546	4.6	0.03755	1.9	0.41	0.14592	4.2	571.4	40.6	237.6	8.8	2,298.7	72.3	58.4	n.d.	n.d.
	153		23	100	0.90703	3.8	0.03936	1.7	0.46	0.16712	3.4	655.5	36.8	248.9	8.4	2,529.0	56.8	62.0	n.d.	n.d.
	154		26	119	0.83752	3.3	0.03831	1.6	0.48	0.15856	2.9	617.8	31.2	242.3	7.6	2,440.4	50.2	60.8	n.d.	n.d.
	155	titanite (external rim zone)	19	124	0.73359	4.4	0.03749	2.0	0.46	0.14192	3.9	558.7	37.7	237.2	9.3	2,250.9	67.1	57.5	n.d.	n.d.
	156		20	131	0.68042	4.5	0.03771	1.8	0.40	0.13086	4.1	527.0	37.5	238.6	8.4	2,109.5	72.9	54.7	n.d.	n.d.
	157		20	128	0.72551	3.9	0.03708	1.6	0.41	0.14191	3.5	553.9	33.4	234.7	7.3	2,250.7	61.4	57.6	n.d.	n.d.
	158		19	119	0.75104	4.6	0.03814	1.8	0.40	0.14282	4.2	568.8	40.2	241.3	8.7	2,261.7	72.6	57.6	n.d.	n.d.
	159		18	122	0.79154	4.6	0.03882	1.9	0.41	0.14789	4.2	592.0	42.1	245.5	9.1	2,321.8	73.0	58.5	n.d.	n.d.
	163		23	121	0.82517	4.3	0.03842	1.8	0.41	0.15577	3.9	610.9	39.9	243.0	8.4	2,410.3	67.0	60.2	n.d.	n.d.
	164		68	409	0.45308	3.0	0.03603	1.2	0.39	0.09120	2.8	379.4	19.1	228.2	5.3	1,450.8	52.7	39.9	n.d.	n.d.
	165		21	132	1.04638	4.0	0.04026	1.6	0.40	0.18850	3.7	727.1	42.1	254.4	8.0	2,729.2	60.9	65.0	n.d.	n.d.
	166		21	132	0.70461	4.1	0.03727	1.6	0.40	0.13712	3.8	541.5	35.0	235.9	7.6	2,191.2	66.2	56.4	n.d.	n.d.
	167		19	148	0.69969	4.6	0.03817	1.6	0.35	0.13295	4.3	538.6	38.7	241.5	7.7	2,137.3	75.3	55.2	n.d.	n.d.
	168	19	126	0.79403	4.3	0.03852	1.4	0.33	0.14950	4.1	593.5	39.5	243.7	6.8	2,340.3	70.6	58.9	n.d.	n.d.	
	169		25	183	0.64632	4.1	0.03778	1.5	0.37	0.12409	3.8	506.2	32.6	239.0	7.1	2,015.9	67.1	52.8	n.d.	n.d.
	170		22	165	0.70375	4.3	0.03734	1.8	0.42	0.13669	3.9	541.0	36.1	236.3	8.3	2,185.7	67.8	56.3	n.d.	n.d.
	171		76	405	0.47834	2.4	0.03593	1.0	0.42	0.09657	2.2	396.9	15.7	227.5	4.5	1,558.9	41.0	42.7	n.d.	n.d.
	173		19	121	0.80402	5.2	0.03884	2.1	0.41	0.15015	4.8	599.1	47.9	245.6	10.3	2,347.7	81.9	59.0	n.d.	n.d.
VRG7425	186	zircon	110	90	0.26723	2.9	0.03563	0.9	0.31	0.05440	2.7	240.5	12.3	225.7	3.9	387.8	61.5	6.2	228.0	5.5
	187		613	1,014	0.35413	1.4	0.03677	0.7	0.49	0.06986	1.2	307.8	7.6	232.8	3.2	924.2	26.1	24.4	233.9	5.0
	188		269	453	0.35170	2.2	0.04026	0.8	0.36	0.06336	2.0	306.0	11.6	254.4	3.9	720.5	43.5	16.9	256.2	5.8
	189		143	163	0.50105	2.2	0.03831	0.9	0.38	0.09485	2.1	412.4	15.2	242.4	4.1	1,525.1	39.2	41.2	244.6	5.9
	190		63	29	0.25208	4.0	0.03671	1.1	0.28	0.04980	3.9	228.3	16.6	232.4	5.2	185.9	90.3	-1.8	235.1	6.4
	191		76	37	0.27668	2.8	0.03580	1.0	0.36	0.05604	2.6	248.0	12.5	226.8	4.5	454.2	58.7	8.6	229.4	5.8
	192		527	1,503	0.26969	1.6	0.03744	0.7	0.45	0.05224	1.4	242.4	6.9	236.9	3.3	296.1	32.8	2.3	238.1	5.1
	193		550	1,240	0.25668	1.6	0.03649	0.7	0.41	0.05102	1.5	232.0	6.7	231.0	3.0	241.6	34.0	0.4	232.2	4.9

(continued)





Continued

Rock Nr.	Spot Nr.	Studied fraction	Isotopic data									Ages							RDC age	
			U (ppm)	Pb (ppm)	²⁰⁷ Pb/ ²³⁵ U	±1σ (%)	²⁰⁶ Pb/ ²³⁸ U	±1σ (%)	rho	²⁰⁷ Pb/ ²⁰⁶ Pb	±1σ (%)	²⁰⁷ Pb/ ²³⁵ U	±2σ (Ma)	²⁰⁶ Pb/ ²³⁸ U	±2σ (Ma)	²⁰⁷ Pb/ ²⁰⁶ Pb	±2σ (Ma)	Disc. (%)	²⁰⁶ Pb/ ²³⁸ U	±2σ (Ma)
	194		455	923	0.25928	1.5	0.03662	0.7	0.45	0.05136	1.3	234.1	6.3	231.8	3.1	256.9	31.2	1.0	233.1	5.0
	195		52	21	0.26020	4.6	0.03607	1.2	0.25	0.05232	4.5	234.8	19.5	228.4	5.3	299.3	102.4	2.7	231.3	6.6
	196		66	33	0.51201	3.2	0.03880	1.2	0.37	0.09571	3.0	419.8	22.0	245.4	5.7	1,542.2	55.8	41.5	248.2	7.1
	197		65	27	0.31322	3.5	0.03551	1.1	0.32	0.06398	3.3	276.7	17.0	224.9	4.9	741.0	70.2	18.7	227.6	6.2
	198		588	476	0.25556	1.5	0.03578	0.7	0.44	0.05180	1.3	231.1	6.2	226.6	2.9	276.6	31.2	1.9	227.9	4.8
	199		145	110	0.29792	2.0	0.03829	0.9	0.43	0.05643	1.8	264.8	9.4	242.2	4.1	469.3	40.6	8.5	244.5	5.9
	203		52	22	1.02762	2.5	0.04170	1.1	0.43	0.17871	2.3	717.7	26.0	263.4	5.6	2,641.0	38.2	63.3	266.5	7.2
	204		784	1,286	0.25988	1.5	0.03602	0.7	0.45	0.05232	1.3	234.6	6.1	228.1	2.9	299.6	30.1	2.7	229.1	4.9
	205		539	1,703	0.26807	1.6	0.03719	0.7	0.42	0.05228	1.5	241.1	7.0	235.4	3.1	297.7	34.2	2.4	236.5	5.0
	206		406	866	0.29035	1.7	0.03628	0.7	0.44	0.05805	1.5	258.8	7.7	229.7	3.3	531.7	33.1	11.3	231.1	4.9
	207		237	336	0.26695	2.0	0.03549	0.7	0.38	0.05456	1.8	240.3	8.4	224.8	3.3	394.2	40.7	6.4	226.6	4.8
	208		63	31	0.25580	3.8	0.03823	1.2	0.31	0.04853	3.6	231.3	15.7	241.8	5.5	125.4	85.0	-4.6	244.7	7.0
	209		251	247	0.25428	2.1	0.03544	0.8	0.35	0.05204	2.0	230.0	8.8	224.5	3.3	287.0	46.1	2.4	226.3	5.1
	210		626	849	0.26920	1.5	0.03631	0.6	0.42	0.05377	1.4	242.1	6.5	229.9	2.9	361.4	31.2	5.0	231.1	4.6
	211		59	23	0.32810	4.1	0.03641	1.2	0.29	0.06536	4.0	288.1	20.8	230.5	5.3	786.1	83.3	20.0	233.3	6.7
	212		228	150	0.25211	2.2	0.03576	0.8	0.35	0.05113	2.1	228.3	9.2	226.5	3.5	246.8	48.5	0.8	228.4	5.2
	213		293	182	0.27302	1.8	0.03559	0.8	0.43	0.05563	1.6	245.1	7.8	225.5	3.4	437.7	36.3	8.0	227.2	5.1
	214		74	48	0.72322	2.9	0.03765	1.2	0.42	0.13931	2.6	552.6	24.9	238.3	5.7	2,218.7	46.0	56.9	240.9	6.9
	215		153	297	0.35895	2.4	0.03658	0.8	0.35	0.07118	2.2	311.4	12.9	231.6	3.8	962.5	45.9	25.6	233.6	5.3
	216		58	22	0.25210	4.0	0.03649	1.1	0.28	0.05011	3.9	228.3	16.6	231.0	5.2	200.1	90.0	-1.2	233.8	6.3
	217		1,464	3,459	0.25582	1.3	0.03640	0.6	0.45	0.05098	1.2	231.3	5.6	230.5	2.8	239.8	28.1	0.4	231.0	4.6
	277		133	130	0.30481	2.5	0.03862	1.0	0.39	0.05724	2.3	270.1	12.1	244.3	4.7	500.8	51.9	9.6	246.6	6.3
	278		1,336	2,526	0.26004	1.4	0.03635	0.6	0.46	0.05189	1.2	234.7	5.7	230.1	2.9	280.5	28.1	1.9	230.8	4.6
	279		512	770	0.25622	1.7	0.03709	0.8	0.45	0.05010	1.6	231.6	7.3	234.8	3.7	199.9	36.5	-1.4	236.1	5.3

Appendix B. Results of U-Pb dating of titanites and zircons from nepheline syenite

Rock Nr.	Spot Nr.	Studied fraction	Isotopic data									Ages						RDC age		
			U (ppm)	Pb (ppm)	²⁰⁷ Pb/ ²³⁵ U	±1σ (%)	²⁰⁶ Pb/ ²³⁸ U	±1σ (%)	rho	²⁰⁷ Pb/ ²⁰⁶ Pb	±1σ (%)	²⁰⁷ Pb/ ²³⁵ U	±2σ (Ma)	²⁰⁶ Pb/ ²³⁸ U	±2σ (Ma)	Disc. (%)	²⁰⁶ Pb/ ²³⁸ U	±2σ (Ma)		
VRG7546	212	titanite	66	155	1.54659	2.8	0.04607	1.6	0.59	0.24346	2.2	949.1	34.5	290.4	9.3	3142.8	36.5	69.4	n.d.	n.d.
	213		31	120	0.77526	4.9	0.03948	2.0	0.41	0.14243	4.4	582.8	43.6	249.6	9.8	2257.0	76.7	57.2	n.d.	n.d.
	214		40	158	0.71918	4.2	0.03807	2.1	0.50	0.13701	3.7	550.2	36.2	240.9	10.0	2189.8	63.9	56.2	n.d.	n.d.
	215		39	165	0.67799	5.3	0.03652	2.2	0.41	0.13464	4.8	525.6	43.7	231.2	9.8	2159.5	84.1	56.0	n.d.	n.d.
	216		37	143	0.74720	4.7	0.03777	2.1	0.45	0.14347	4.2	566.6	41.6	239.0	9.9	2269.6	73.4	57.8	n.d.	n.d.
	217		41	137	0.86524	3.6	0.04055	1.9	0.53	0.15474	3.1	633.0	34.4	256.3	9.7	2399.0	52.6	59.5	n.d.	n.d.
	218		38	137	1.64935	3.3	0.04719	1.9	0.60	0.25350	2.6	989.3	41.6	297.2	11.3	3206.8	41.9	70.0	n.d.	n.d.
	219		25	127	0.67242	5.8	0.03860	2.5	0.42	0.12634	5.3	522.2	48.0	244.2	11.8	2047.7	93.2	53.2	n.d.	n.d.
	223		24	137	0.71374	5.1	0.03837	2.1	0.42	0.13492	4.6	547.0	43.6	242.7	10.2	2163.1	81.1	55.6	n.d.	n.d.
	224		55	223	0.74245	3.6	0.03774	1.6	0.46	0.14266	3.2	563.8	31.0	238.8	7.7	2259.8	54.7	57.6	n.d.	n.d.
	225		75	289	0.68795	3.2	0.03925	1.5	0.48	0.12712	2.8	531.6	26.7	248.2	7.5	2058.5	49.9	53.3	n.d.	n.d.
	226		27	121	0.70438	5.1	0.03791	2.1	0.41	0.13477	4.6	541.4	43.2	239.8	9.9	2161.1	81.2	55.7	n.d.	n.d.
	227		24	130	0.85630	5.4	0.03958	2.5	0.46	0.15689	4.8	628.1	51.3	250.3	12.2	2422.5	81.8	60.2	n.d.	n.d.
	228		24	134	0.77055	5.3	0.03900	2.1	0.40	0.14330	4.8	580.1	47.2	246.6	10.3	2267.5	83.5	57.5	n.d.	n.d.
	229		20	117	0.72592	5.8	0.03821	2.3	0.39	0.13780	5.4	554.2	50.6	241.7	10.9	2199.7	93.6	56.4	n.d.	n.d.
	230		50	160	0.68620	4.1	0.03795	1.9	0.46	0.13113	3.6	530.5	34.3	240.1	9.0	2113.2	64.2	54.7	n.d.	n.d.
	231		37	138	0.71482	5.3	0.03725	2.3	0.45	0.13916	4.7	547.6	45.0	235.8	10.9	2216.9	81.9	56.9	n.d.	n.d.
	232		32	128	0.61333	4.2	0.03810	2.0	0.46	0.11676	3.7	485.7	32.9	241.0	9.3	1907.3	67.6	50.4	n.d.	n.d.
	233		22	120	2.14270	3.9	0.05327	2.2	0.55	0.29170	3.3	1162.7	55.2	334.6	14.2	3426.7	51.5	71.2	n.d.	n.d.
	234		21	118	0.73199	6.4	0.03692	2.3	0.36	0.14380	6.0	557.7	55.5	233.7	10.5	2273.5	102.8	58.1	n.d.	n.d.
	235		21	114	0.66111	6.3	0.03738	2.2	0.34	0.12829	5.9	515.3	51.6	236.5	10.1	2074.7	104.5	54.1	n.d.	n.d.
	236		31	122	0.67883	4.9	0.03804	2.2	0.45	0.12944	4.4	526.1	41.0	240.6	10.6	2090.4	77.6	54.3	n.d.	n.d.
	237		50	167	1.04936	3.1	0.04245	1.9	0.60	0.17929	2.5	728.6	32.7	268.0	9.8	2646.4	42.0	63.2	n.d.	n.d.
	238		50	173	0.74667	3.7	0.03987	1.6	0.44	0.13581	3.3	566.3	32.3	252.1	7.9	2174.5	58.2	55.5	n.d.	n.d.
	239		47	169	0.75969	3.8	0.03881	1.7	0.44	0.14197	3.4	573.8	33.3	245.5	8.0	2251.4	58.7	57.2	n.d.	n.d.
	2	zircon	163	123	0.29791	3.1	0.03647	1.1	0.35	0.05924	2.9	264.8	14.4	230.9	4.9	575.8	63.0	12.8	233.0	6.3
	8		719	588	0.25134	1.7	0.03622	0.7	0.38	0.05032	1.6	227.7	7.1	229.4	3.0	209.7	37.5	-0.8	230.6	4.9
	9		396	183	0.25785	2.6	0.03641	0.8	0.30	0.05136	2.5	232.9	10.8	230.6	3.5	257.0	56.8	1.0	232.1	5.2
	10		260	115	0.25341	2.6	0.03638	1.0	0.38	0.05051	2.4	229.3	10.5	230.4	4.4	218.7	55.0	-0.5	232.2	5.9
	11		758	481	0.25583	2.0	0.03731	0.8	0.38	0.04973	1.8	231.3	8.2	236.1	3.5	182.5	43.0	-2.1	237.3	5.4
	12		122	87	0.35852	3.5	0.03783	1.4	0.39	0.06873	3.3	311.1	19.1	239.4	6.6	890.6	67.5	23.0	241.7	7.7
	13		815	825	0.25133	1.9	0.03642	0.7	0.37	0.05005	1.8	227.7	7.9	230.6	3.2	197.4	41.8	-1.3	231.7	4.9
	14		273	411	0.39439	2.4	0.04008	1.0	0.43	0.07136	2.1	337.6	13.6	253.4	5.1	967.8	43.9	24.9	255.1	6.5
	15		2338	4194	0.25599	1.4	0.03642	0.6	0.40	0.05098	1.3	231.4	6.0	230.6	2.7	239.8	30.8	0.4	230.9	4.6
	16		632	830	0.30083	2.1	0.03800	0.7	0.33	0.05740	2.0	267.1	10.0	240.5	3.3	507.1	44.2	10.0	241.7	5.1
	17		513	370	0.25407	1.8	0.03636	0.9	0.47	0.05067	1.6	229.9	7.5	230.3	3.9	226.0	37.6	-0.2	231.6	5.6
	18		346	190	0.23856	2.3	0.03601	0.8	0.35	0.04804	2.1	217.2	9.0	228.1	3.6	101.3	51.0	-5.0	229.7	5.2
	19		58	19	0.27159	5.7	0.03527	1.6	0.28	0.05585	5.5	244.0	24.8	223.4	7.1	446.4	121.3	8.4	226.2	8.0
	20		58	22	0.25220	5.1	0.03528	1.4	0.28	0.05185	4.9	228.4	21.1	223.5	6.3	278.6	113.1	2.1	226.2	7.2
	21		614	566	0.28735	2.0	0.03626	0.7	0.35	0.05747	1.8	256.5	8.9	229.6	3.1	509.7	40.5	10.5	230.9	4.9
	22		428	336	0.24654	2.3	0.03588	0.8	0.35	0.04983	2.1	223.8	9.2	227.3	3.6	187.1	49.8	-1.6	228.7	5.2
	27		303	235	0.34566	2.3	0.03696	0.8	0.35	0.06783	2.2	301.5	12.3	234.0	3.8	863.3	45.9	22.4	235.7	5.3

(continued)





Continued

Rock Nr.	Spot Nr.	Studied fraction	Isotopic data									Ages						RDC age		
			U (ppm)	Pb (ppm)	²⁰⁷ Pb/ ²³⁵ U	±1σ (%)	²⁰⁶ Pb/ ²³⁸ U	±1σ (%)	rho	²⁰⁷ Pb/ ²⁰⁶ Pb	±1σ (%)	²⁰⁷ Pb/ ²³⁵ U	±2σ (Ma)	²⁰⁶ Pb/ ²³⁸ U	±2σ (Ma)	²⁰⁷ Pb/ ²⁰⁶ Pb	±2σ (Ma)	Disc. (%)	²⁰⁶ Pb/ ²³⁸ U	±2σ (Ma)
	28		145	84	0.83472	2.0	0.04177	1.2	0.62	0.14493	1.6	616.2	18.8	263.8	6.4	2287.0	28.2	57.2	266.2	7.6
	29		684	358	0.26225	1.7	0.03752	0.6	0.36	0.05069	1.6	236.5	7.1	237.4	2.8	227.0	36.4	-0.4	238.7	4.8
	30		883	534	0.26774	1.8	0.03691	0.7	0.37	0.05260	1.7	240.9	7.8	233.7	3.1	311.8	38.6	3.0	234.7	5.0
	31		187	97	0.25814	2.9	0.03574	1.0	0.36	0.05238	2.7	233.2	12.1	226.4	4.7	302.0	61.8	2.9	228.4	5.8
	32		410	245	0.25477	2.3	0.03615	0.7	0.32	0.05111	2.2	230.4	9.5	229.0	3.3	245.7	50.3	0.6	230.5	4.9
	33		321	213	0.24952	2.6	0.03669	0.9	0.33	0.04932	2.4	226.2	10.5	232.3	3.9	163.0	57.1	-2.7	234.0	5.6
	34		356	321	0.25461	2.6	0.03638	0.7	0.26	0.05075	2.5	230.3	10.6	230.4	3.0	229.6	57.5	0.0	232.0	4.9
	35		329	318	0.25435	2.4	0.03601	0.9	0.35	0.05123	2.3	230.1	10.1	228.1	3.8	251.1	52.7	0.9	229.7	5.5
	36		182	158	0.24532	3.5	0.03471	1.0	0.29	0.05125	2.6	222.8	14.0	220.0	4.3	252.2	76.9	1.2	221.9	5.7
	37		295	375	0.24633	2.8	0.03531	0.9	0.34	0.05060	2.6	223.6	11.2	223.7	4.2	222.6	60.5	0.0	225.3	5.4
	38		205	215	0.29938	2.8	0.03565	0.8	0.30	0.06091	2.6	265.9	12.9	225.8	3.7	636.0	56.6	15.1	227.7	5.1
	39		978	796	0.26487	1.8	0.03655	0.7	0.36	0.05255	1.7	238.6	7.7	231.5	3.0	309.3	38.4	3.0	232.4	4.9
	40		1064	845	0.25724	1.6	0.03617	0.7	0.41	0.05157	1.5	232.4	6.8	229.1	3.0	266.4	34.5	1.4	230.0	4.9
	41		779	825	0.25774	1.6	0.03640	0.7	0.47	0.05135	1.4	232.8	6.5	230.5	3.4	256.7	32.1	1.0	231.6	4.9
	42		167	39	0.27072	3.2	0.03657	1.0	0.32	0.05369	3.1	243.3	14.0	231.5	4.7	358.1	69.3	4.8	233.7	6.0
	47		213	58	0.24678	3.2	0.03625	0.9	0.28	0.04936	3.1	224.0	13.1	229.6	4.2	165.2	72.7	-2.5	231.6	5.6
	48		65	23	0.26598	4.4	0.03566	1.5	0.33	0.05410	4.1	239.5	18.7	225.9	6.5	375.1	92.6	5.7	228.6	7.7
	49		65	26	0.28945	4.6	0.03597	1.2	0.26	0.05835	4.5	258.1	21.2	227.9	5.4	542.9	97.9	11.7	230.6	6.6
	50		235	191	0.25644	2.5	0.03552	0.8	0.33	0.05236	2.4	231.8	10.4	225.0	3.6	301.2	54.3	2.9	226.8	5.1
	51		571	720	0.25764	2.0	0.03677	0.7	0.36	0.05082	1.9	232.8	8.5	232.8	3.3	232.5	44.1	0.0	234.0	5.0
	52		551	677	0.24864	2.0	0.03646	0.7	0.34	0.04946	1.9	225.5	8.0	230.9	3.0	169.6	43.6	-2.4	232.1	4.9
	53		306	147	0.25863	2.5	0.03588	0.8	0.30	0.05227	2.4	233.6	10.6	227.3	3.5	297.1	55.3	2.7	229.0	5.2
	54		315	198	0.24386	2.1	0.03561	0.9	0.40	0.04966	1.9	221.6	8.5	225.6	3.8	179.0	45.6	-1.8	227.3	5.5
	55		133	51	0.25036	3.7	0.03603	1.1	0.29	0.05039	3.6	226.9	15.2	228.2	4.9	213.2	82.7	-0.6	230.5	6.2
	56		577	1293	0.26913	2.1	0.03632	0.8	0.39	0.05373	1.9	242.0	9.0	230.0	3.7	359.8	43.8	4.9	231.2	5.2
	57		219	189	0.25893	2.7	0.03533	0.9	0.34	0.05315	2.5	233.8	11.3	223.8	4.0	335.4	57.7	4.3	225.7	5.4
	58		429	253	0.25053	2.1	0.03627	0.9	0.44	0.05010	1.9	227.0	8.7	229.7	4.2	199.6	44.4	-1.2	231.2	5.5
	59		216	197	0.25083	3.0	0.03587	0.9	0.30	0.05071	2.9	227.3	12.4	227.2	4.1	227.8	67.2	0.0	229.1	5.5
	60		361	220	0.25474	2.0	0.03617	0.8	0.37	0.05107	1.9	230.4	8.4	229.1	3.4	244.2	43.8	0.6	230.7	5.2
	61		519	375	0.25554	2.1	0.03596	0.7	0.33	0.05154	2.0	231.1	8.7	227.7	3.1	265.1	45.9	1.4	229.1	4.9
	62		384	256	0.27256	2.3	0.03625	0.7	0.33	0.05452	2.2	244.7	10.0	229.6	3.4	392.8	48.6	6.2	231.1	4.9
	66		27	12	1.10886	4.5	0.12338	1.3	0.30	0.06518	4.7	757.6	48.7	750.0	19.1	780.2	90.6	1.0	757.8	22.1
	67		303	166	0.24457	2.6	0.03599	0.8	0.31	0.04927	2.5	222.2	10.5	228.0	3.6	161.0	58.5	-2.6	229.7	5.2
	68		483	803	0.25976	1.8	0.03710	0.7	0.42	0.05077	1.6	234.5	7.5	234.9	3.4	230.6	37.6	-0.2	236.2	5.0
	69		248	170	0.24450	3.1	0.03592	1.0	0.31	0.04936	2.9	222.1	12.4	227.6	4.3	164.8	68.8	-2.5	229.4	5.8
	70		69	28	0.28168	4.8	0.03614	1.5	0.30	0.05652	4.6	252.0	21.6	228.9	6.6	472.9	101.7	9.2	231.6	7.8
	71		126	70	0.26269	3.5	0.03634	1.1	0.33	0.05242	3.3	236.8	14.7	230.1	5.1	303.9	74.9	2.8	232.4	6.3
	72		967	1462	0.25258	1.7	0.03593	0.8	0.44	0.05098	1.5	228.7	7.0	227.6	3.4	239.8	35.8	0.5	228.5	5.2
	73		296	284	0.26067	2.4	0.03706	0.8	0.34	0.05101	2.3	235.2	10.2	234.6	3.8	241.2	52.6	0.3	236.3	5.3
	74		143	51	0.24486	3.3	0.03552	1.2	0.37	0.04999	3.0	222.4	13.1	225.0	5.3	194.6	70.9	-1.2	227.2	6.5
	75		696	688	0.26251	1.9	0.03601	0.7	0.39	0.05287	1.7	236.7	7.9	228.1	3.3	323.3	39.2	3.6	229.2	4.9
	76		149	28	0.24971	3.7	0.03543	1.1	0.29	0.05111	3.5	226.3	15.0	224.5	4.7	245.7	81.1	0.8	226.7	6.1
	77		890	424	0.24788	1.7	0.03577	0.7	0.41	0.05025	1.6	224.9	7.0	226.6	3.2	206.6	37.0	-0.8	227.7	4.8
	78		446	121	0.25187	2.0	0.03572	0.8	0.38	0.05113	1.9	228.1	8.3	226.3	3.5	246.9	43.6	0.8	227.8	5.1
	79		378	102	0.26057	2.2	0.03704	0.9	0.38	0.05102	2.1	235.1	9.5	234.5	4.0	241.6	48.0	0.3	236.1	5.7
	80		517	711	0.24154	2.1	0.03541	0.7	0.35	0.04947	1.9	219.7	8.1	224.3	3.2	170.2	45.0	-2.1	225.6	4.8
	81		859	922	0.26900	1.8	0.03631	0.7	0.37	0.05372	1.7	241.9	7.7	230.0	3.0	359.5	37.9	4.9	231.0	4.9

(continued)

Continued

Rock Nr.	Spot Nr.	Studied fraction	Isotopic data								Ages						RDC age			
			U (ppm)	Pb (ppm)	²⁰⁷ Pb/ ²³⁵ U	±1σ (%)	²⁰⁶ Pb/ ²³⁸ U	±1σ (%)	rho	²⁰⁷ Pb/ ²⁰⁶ Pb	±1σ (%)	²⁰⁷ Pb/ ²³⁵ U	±2σ (Ma)	²⁰⁶ Pb/ ²³⁸ U	±2σ (Ma)	²⁰⁷ Pb/ ²⁰⁶ Pb	±2σ (Ma)	Disc. (%)	²⁰⁶ Pb/ ²³⁸ U	±2σ (Ma)
	82		810	882	0.25301	1.8	0.03571	0.7	0.39	0.05137	1.7	229.0	7.5	226.2	3.2	257.6	39.1	1.2	227.3	4.8
	347		788	843	0.25886	1.9	0.03673	1.0	0.50	0.05112	1.7	233.7	8.0	232.5	4.3	246.3	38.5	0.5	233.6	6.0
	348		220	104	0.26570	2.6	0.03712	1.1	0.42	0.05192	2.3	239.3	11.0	234.9	5.0	282.0	53.9	1.8	236.9	6.4
	349		540	409	0.25685	2.1	0.03729	1.0	0.46	0.04995	1.8	232.1	8.6	236.0	4.5	192.9	43.0	-1.7	237.4	6.0
	350		538	443	0.25604	2.0	0.03610	0.9	0.46	0.05143	1.8	231.5	8.4	228.6	4.2	260.4	41.5	1.2	230.0	5.5
	351		1138	547	0.25040	1.9	0.03584	1.0	0.51	0.05067	1.6	226.9	7.6	227.0	4.3	225.9	37.4	0.0	227.9	5.8
	352		1209	661	0.26116	1.8	0.03589	0.9	0.49	0.05277	1.6	235.6	7.7	227.3	4.0	319.0	36.8	3.5	228.2	5.5
	353		1102	564	0.25674	1.8	0.03638	1.0	0.53	0.05118	1.6	232.0	7.6	230.4	4.4	249.0	36.1	0.7	231.3	5.9
	354		286	286	0.24608	2.7	0.03603	1.1	0.42	0.04953	2.5	223.4	10.9	228.2	5.0	173.0	57.5	-2.2	229.9	6.2
	355		435	494	0.26319	2.3	0.03680	1.0	0.43	0.05187	2.1	237.2	9.7	233.0	4.5	279.6	47.5	1.8	234.4	6.0
	356		134	46	0.26488	3.8	0.03556	1.1	0.30	0.05402	3.6	238.6	16.0	225.3	5.0	371.8	80.7	5.6	227.5	6.2
	358		252	255	0.25008	2.5	0.03630	1.0	0.40	0.04997	2.3	226.6	10.3	229.9	4.6	193.5	54.2	-1.4	231.6	5.9
	359		168	74	0.24981	3.2	0.03608	1.1	0.33	0.05022	3.0	226.4	13.0	228.5	4.7	205.1	70.2	-0.9	230.6	6.2
	364		150	69	0.16750	4.8	0.03571	1.2	0.24	0.03402	4.6	157.3	14.0	226.2	5.2	0.1	0.0	-43.8	228.3	6.5
	365		412	304	0.24596	2.6	0.03548	1.1	0.41	0.05029	2.4	223.3	10.5	224.7	4.8	208.3	55.2	-0.6	226.2	6.1
	367		120	66	0.21858	4.1	0.03522	1.2	0.30	0.04501	3.9	200.7	14.9	223.1	5.4	0.1	0.2	-11.2	225.4	6.5
	368		447	299	0.24771	2.7	0.03657	1.2	0.43	0.04913	2.5	224.7	11.0	231.5	5.3	154.0	57.8	-3.0	233.0	6.7
	369		300	215	0.25628	2.9	0.03739	1.1	0.38	0.04971	2.7	231.7	12.2	236.6	5.2	181.7	63.3	-2.1	238.4	6.4
	370		419	377	0.25357	2.1	0.03715	1.0	0.47	0.04951	1.9	229.5	8.8	235.1	4.6	172.1	44.3	-2.5	236.6	6.0
	371		755	596	0.25527	2.2	0.03588	1.0	0.46	0.05160	1.9	230.8	9.0	227.2	4.5	267.8	44.6	1.6	228.4	5.8
	372		1302	1870	0.26212	1.8	0.03642	0.9	0.49	0.05221	1.6	236.4	7.7	230.6	4.1	294.5	36.5	2.5	231.3	5.5
	373		321	221	0.26007	2.7	0.03058	1.1	0.41	0.06167	2.5	234.7	11.5	194.2	4.3	662.8	53.5	17.3	195.7	5.3
	374		508	322	0.25522	2.2	0.03647	1.0	0.48	0.05075	1.9	230.8	9.0	230.9	4.8	229.7	44.1	0.0	232.3	5.9
	375		447	260	0.25287	2.4	0.03598	1.0	0.41	0.05097	2.2	228.9	9.8	227.9	4.4	239.5	50.2	0.4	229.4	5.8
	376		845	506	0.25212	2.0	0.03588	0.9	0.46	0.05096	1.7	228.3	8.0	227.3	4.0	239.0	40.1	0.5	228.3	5.5
	377		226	131	0.27130	4.0	0.03662	1.2	0.31	0.05373	3.8	243.7	17.3	231.9	5.5	359.9	85.4	4.9	233.8	6.7
	378		747	454	0.25565	2.0	0.03654	0.9	0.46	0.05074	1.8	231.2	8.4	231.4	4.2	229.0	41.9	-0.1	232.5	5.6
	379		390	247	0.24105	2.6	0.03581	1.0	0.38	0.04882	2.4	219.3	10.5	226.8	4.5	139.1	57.6	-3.4	228.4	5.8
	383		368	134	0.25856	2.2	0.03557	1.0	0.46	0.05272	2.0	233.5	9.2	225.3	4.4	316.6	44.7	3.5	226.9	5.8
	384		353	154	0.24551	2.6	0.03595	1.0	0.37	0.04954	2.5	222.9	10.6	227.7	4.3	173.4	57.3	-2.1	229.3	5.8
	385		210	109	0.24320	3.3	0.03443	1.2	0.35	0.05124	3.1	221.0	13.3	218.2	5.0	251.5	71.8	1.3	220.1	6.3
	386		181	41	0.26851	3.4	0.03588	1.1	0.31	0.05427	3.2	241.5	14.6	227.3	4.7	382.4	72.5	5.9	229.3	6.2
	387		219	154	0.24940	3.4	0.03547	1.3	0.38	0.05100	3.1	226.1	13.9	224.7	5.8	240.9	72.6	0.6	226.6	6.9
	388		56	19	0.19895	7.6	0.03552	1.6	0.22	0.04063	7.4	184.2	25.7	225.0	7.2	0.1	0.1	-22.1	227.8	8.1
	389		355	452	0.27273	2.5	0.03676	1.0	0.41	0.05380	2.2	244.9	10.8	232.7	4.6	362.8	50.9	5.0	234.4	6.0
	390		65	27	0.27183	4.7	0.03519	1.7	0.37	0.05602	4.3	244.2	20.3	223.0	7.6	453.2	96.1	8.7	225.6	8.4
	391		61	23	0.25265	6.6	0.03455	1.5	0.23	0.05303	6.5	228.7	27.4	219.0	6.6	330.3	146.5	4.3	221.6	7.5
	392		66	22	0.22581	5.2	0.03558	1.4	0.28	0.04603	5.0	206.7	19.5	225.4	6.4	0.1	9.6	-9	228.1	7.3
	393		179	199	0.26902	3.6	0.03580	1.1	0.30	0.05451	3.4	241.9	15.4	226.7	4.8	392.1	76.3	6.3	228.7	6.2
	394		253	307	0.24991	3.1	0.03537	1.1	0.36	0.05125	2.9	226.5	12.8	224.0	5.0	252.2	67.6	1.1	225.8	6.1
	395		145	69	0.24820	3.4	0.03574	1.2	0.36	0.05037	3.2	225.1	13.8	226.4	5.4	212.2	73.8	-0.6	228.5	6.5

